UNIVERSITÀ DI PISA

Dipartimento di Farmacia

Corso di Laurea Specialistica in Farmacia

Design and synthesis of novel probes for TSPO featuring an isoquinolinecarboxamide or quinazolinecarboxamide scaffold

Relatori:

Dott.ssa Sabrina Taliani

Dott.ssa Elisabetta Barresi

Candidata:

Cecilia Lombardi

Anno Accademico 2012/2013

INDEX

INTRODUCTION

The Translocator Protein (TSPO), has been first identified in 1977 as binding site for the benzodiazepine diazepam in peripheral tissues (PBR). The early characterization of these "diazepam binding sites" outside the brain led to their nomination as "Peripheral-type benzodiazepine receptor", to distinguish them from the central benzodiazepine receptor (CBR) which is part of the γ-aminobutyric acid (GABA) type A ($GABA_A$) receptor complex[1,2]. Benzodiazepines widespread use in clinic is based upon potent anxiolytic, anticonvulsivant, hypnotic, muscle-relaxant and sedative properties, actions mediated by CBR that is restricted to the central nervous system (CNS)[3].

In 2006, Papadopoulos and co-workers[4] renamed the PBR to Translocator Protein (18 kDa), with the abbreviation "TSPO". The renaming of this protein was thought to represent more accurately findings regarding its structure, subcellular roles and putative functions. Further review of the current literature highlights the following key reasons and rationale that support this name change for the PBR.

(i) The term 'benzodiazepine' is inaccurate because many ligands of other structures, such as cholesterol and protoporphyrin IX, also bind to the PBR. In addition, not all benzodiazepines bind to the PBR, so that including 'benzodiazepine' in the nomenclature is potentially misleading and inaccurate.

(ii) The term 'peripheral-type' does not reflect the real tissue distribution of the PBR because it is also expressed in glial and ependymal cells, which are located in the CNS.

(iii) The PBR protein itself is not a receptor in the traditional sense. Cellular localization is usually, even though not always, mitochondrial. Although some data indicate that extra mitochondrial localizations of the PBR could result from mutations, there are no data indicating common functions of the nuclear and mitochondrial fractions.

(iv) The term 'binding site' does not define the function with adequate specificity; binding *per se* does not reflect the importance of the protein or receptor, and it is too general term.

(v) Although 'receptor' functionality is appealing in the context of cell signalling, it might not be an optimal descriptor given the diverse nature of candidate physiological and pharmacological ligands and the currently incomplete understanding of the potential role of the PBR protein in the transduction of cell signals.

There are three main Structure Activity Relationships (SAR) for the TSPO: (i) cholesterol binding and transport; (ii) protein import; and (iii) porphyrin binding and transport. Given all of these considerations, the expert panel reached a consensus to recommend renaming the PBR to TSPO.[4]

The TSPO is an evolutionarily well-conserved 18 kDa protein consisting of 169 amino acids,[2] which is mainly located at the contact sites between the outer and inner mitochondrial membranes,[5] although it is also expressed at low levels in other subcellular compartments, such as plasma membranes and nuclear fraction of cells.[4] In mitochondria, the three-dimensional structure of TSPO, which is highly hydrophobic and rich in tryptophan, is characterized by five α-helices spanning through the phospholipids bilayer of the mitochondrial membrane. Photolabelling studies indicated that this receptor is strictly associated in a trimeric complex with the 32 kDa voltage-dependent anion channel (VDAC) and the 30 kDa adenine nucleotide translocase (ANT), to constitute the mitochondrial permeability transition pore (MPTP), **Figure 1.**

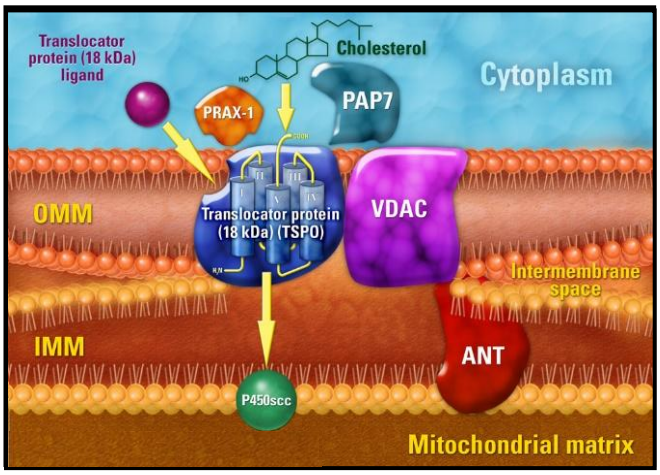

Figure 1. Translocator Protein.[4]

To date, four cytosolic TSPO interacting proteins have been identified, the function of two of them being unknown: PRAX-1, which interacts with the C-terminal end of TSPO and p10, a 10 kDa protein which was co-immunoprecipitated with the TSPO, but whose identity has not been unravelled.[6] The two other TSPO partners are the steroidogenic acute regulatory protein, StAR, which binds cholesterol and promotes mitochondrial cholesterol transfer[7] and PKA-associated protein 7, PAP7, which regulates steroidogenesis as shown in antisense and overexpression studies.[6,8]

Varieties of endogenous molecules with different chemical structures that bind to TSPO have been identified. Among these, the main endogenous ligands include protoporphyrins (protoporphyrin IX, mesoporphyrin IX, deuteroporphyrin IX, hemin), phospholipase A2 (PLA2), diazepam binding inhibitor (DBI), and its biologically active derivatives.[9] Cholesterol is also considered an endogenous nanomolar affinity ligand for TSPO.

TSPO is widely expressed throughout the body, with higher levels in steroid producing tissues, but also in other peripheral tissues including liver, heart, kidney, lung, immune system. In the CNS, TSPO is mainly located in glial and ependymal cells.[4]

TSPO is involved in a variety of biological processes including cholesterol transport, steroidogenesis, calcium homeostasis, lipid metabolism, mitochondrial oxidation, cell growth and differentiation, apoptosis induction, and regulation of immune functions.[10,11]

TSPO and Regulation of Steroidogenesis

Biosynthesis of tissue specific steroids typically involves the conversion of cholesterol into pregnenolone, which occurs through cholesterol side chain cleavage by cytochrome P450 enzyme (P450scc) and auxiliary electron transferring proteins, localized on the inner mitochondrial membrane. Cholesterol transport from the outer to the inner mitochondrial membrane is the

rate-determining step in steroid and bile acid syntheses.[12,13] Widespread studies on the location and function of TSPO have found its role to be primarily involved in the cholesterol transport through the mitochondrial membranes and thus in the steroid synthesis. Cholesterol transport from the outer to the inner mitochondrial membrane is activated by specific ligand binding to TSPO, after which cholesterol undergoes metabolism and begins the steroidogenesis cascade.[4] Cholesterol may interact with a receptor binding site on the C-terminus of the TSPO[14], triggering its transport from the outer to the inner mitochondrial membranes.[13,15] In the inner mitochondrial membrane, cholesterol is converted to pregnenolone by the C27 cholesterol side chain cleavage cytochrome P450 enzyme (P450scc), that catalyses a series of reactions involving the formation of the 22*R*-hydroxycholesterol and 20,22*R*-hydroxycholesterol intermediates, followed by cleavage of the bond between C20 and C22. Pregnenolone then leaves the mitochondrion to undergo enzymatic transformation in the endoplasmic reticulum that will give rise to the final steroid products,[16] **Figure 2.**

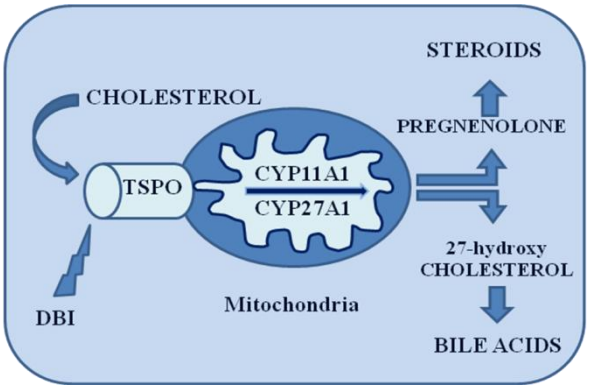

Figure 2. Cholesterol metabolism in hepatic and steroidogenic cells. Cholesterol binds to TSPO and its transported up on binding of endozepine also called DBI. In hepatic cells, cholesterol is hydroxylated by cytochrome P450 (CYP27A1) to give 27-hydroxycholesterol, whereas in steroidogenic cells, cholesterol is cleavage by another cytochrome P450 (CYP11A1) that cleave side chain to give pregnenolone.

TSPO and Apoptosis

The apoptotic cascade leading to cell death has been well characterized and in this process the dissipation of the mitochondrial transmembrane potential caused by the opening of the MPTP represent a critical initiating event. The resulting increased volume in the mitochondrial matrix leads to the disruption of the outer membrane integrity and the release of intermembrane proteins from the mitochondria. These proteins include cytocrome c and the apoptosis inducing factor, AIF. The AIF is a flavoprotein that translocates to the nucleus where it induces nuclear chromatin condensation and a large scale DNA fragmentation. In the cytosol, the cytochrome c interacts with Apaf-1 (apoptosis activating factor 1) and pro-caspase 9, leading to the activation of caspase 9, which in turn cleaves pro-caspase 3 to yield active caspase 3. This caspase activates a range of enzymes critical for inducing the structural rearrangement of the nucleus, cytoskeleton and plasma membrane that are characteristic of apoptosis.[6] Apoptosis is defined as the transient opening of MPTP, as reclosure of the pore ensuring this transient process does not result in necrosis and ATP levels are ultimately maintained inside the cell.[13] TSPO is an endogenous modulator of this process but the exact mechanism has not yet been definitively established. TSPO regulation may act at different levels and some proposed mechanisms include the modulation of the MPTP or the direct interaction with pro- or anti-apoptotic molecules.[6]

In 2007 Li and co-workers[17] showed that the specific TSPO ligand PK11195[18] induces mitochondrial release of cytochrome c and ultimately induced mitochondrial uncoupling. PK11195 also facilitates the induction of apoptosis, reverses Bcl-2-mediated inhibition of apoptosis, and facilitates TNF-R-induced necrosis, producing a multicomponent effect on the induction of cell death. Outline, it is important to note that the proapoptotic effects of PK11195 are significant only at concentrations 1000-fold higher that those required for specific binding to TSPO.[13]

TSPO and Immunomodulation

The presence of TSPO in a wide range of immunomodulatory cells such as microglia, blood monocytes, lymphocytes, and leukocytes implies its involvement in immune response. The mechanism through which this occurs is largely unknown. Macrophages express high levels of TSPO binding sites and, in mouse studies, TSPO ligands, specifically benzodiazepines, inhibit the capacity of macrophages to produce ROS and inflammatory cytokines such as IL-1, TNFR, and IL-6. Furthermore, TSPO is involved in the regulation of phagocyte oxidative metabolism, a process that is normally required for inducing effective elimination of foreign antigens. This immunosuppressive function of some TSPO ligands suggests an important role in host defense mechanisms and inflammatory response.

In the health CNS, TSPO is minimally expressed on microglial cells. Upon the injection of excitotoxic compounds, there occurs a dose-dependent increase in the level of TSPO, an up-regulation closely correlated with microglial activation. Inflammatory mechanisms initiated by microglia are implicated as part of the primary and secondary mechanisms of inflammatory neurodegenerative diseases, such as Alzheimer's disease (AD),[19] whereby the activation of microglia initiates an inflammatory response that may exacerbate neuronal damage. The inflammation that occurs in the brain during such neurodegenerative diseases is thought to involve TSPO through its increased presence in activated microglia, thus presenting the possibility for the use of specific TSPO ligands to prevent or limit neuroinflammation. However, the involvement of activated microglia in different CNS diseases differs with respect to its role in disease progression and severity. By use of TSPO as a marker for activated microglia, it is possible to determine exactly what role the neuroinflammation plays in specific CNS disease states, opening doors for treatment or inhibition of disease progression.[13]

The TSPO Altered Expression

TSPO basal expression is up-regulated in a number of human pathologies, including a variety of tumors and neuropathologies, such as gliomas and neurodegenerative disorders (Huntington's and Alzheimer's diseases), as well as various forms of brain injury and inflammation.[20,21,22] Furthermore, changes in TSPO receptor levels were found in anxiety and mood disorders.[9,23,24] Recent evidences suggest that TSPO on glial cells may regulate the biosynthesis of neurosteroids, leading to the hypothesis of its potential role as key determinant for the treatment of neuropathological conditions.[7,13]

TSPO in Cancer

The recent literature on TSPO includes many reports dealing with TSPO and cancer. The rationale behind the potential application of TSPO-targeted therapies in cancer is based on two main features: i) alteration of TSPO expression in tumor cells and ii) TSPO-dependent apoptosis modulations. Considering TSPO expression, some of highest densities of TSPO are observed in neoplastic tissues and cell lines. Ovarian, hepatic and colon carcinomas, adenocarcinoma, and glioma all show increased TSPO densities relative to untransformed tissues. Even higher levels of TSPO density were observed in more rapidly proliferating breast cancer cells and more aggressive breast cancer phenotypes. In further, an important relationship between TSPO expression, proliferation rate and tumor aggressivity was recently documented by Hardwich and co-workers.[25] These data suggest that monitoring TSPO expression may be relevant in the clinic and that the protein could be used as a diagnostic and/or prognostic marker. Some TSPO ligands may have potential as antitumor molecules which would be related to their antiproliferative and pro-apoptotic properties. Consistent with this, FGIN-1-27[26] and PK11195[18] were shown to have antitumoral activities and to induce apoptosis and cell cycle arrest in colorectal

and esophageal cancer cell lines, and cancer primary cell cultures. These observations indicate that TSPO is an attractive target in cancer therapy.[6]

TSPO in Inflammation and Auto-Immune Diseases

TSPO is also involved in the regulation of immune responses. In the immune system, TSPO is widely expressed: in the thymus, where the protein is restricted to the medulla, in the white pulp of the spleen, in the lymph nodes, in the Peyer patches of the intestine and in all human peripheral blood leukocyte subsets. As observed for tumoral cell lines, changes in TSPO expression have already been associated with several inflammatory conditions: PK11195 binding is up-regulated in experimental autoimmune encephalitis, motor neuron axotomy, sciatic nerve degeneration and regeneration.[27] TSPO ligands exhibit anti-inflammatory properties. They modulate monocyte chemotaxis and humoral responses such as macrophage production of reactive oxygen intermediates, TNF, or IL-1 and IL-6.[28] Both Ro5-4864 and PK11195 were show to limit the severity and progression of different inflammatory processes. For instance, they were highly potent at inhibiting inflammatory signs in two mouse models of acute inflammation, where a treatment with carrageenan induced a paw oedema formation and pleurisy.[29] The potential therapeutic benefit of TSPO ligands is not restricted to arthritis treatment and may be enlarged to other auto-immune pathologies. The protective effect of Ro5-4864, PK11195 and SSR180575 was also demonstrated in a spontaneous inflammatory skin pathology developed in an *in vivo* model of lupus erythematosus.[30] These examples support the rationale that targeting TSPO may have beneficial effect in the treatment of inflammatory disorders and auto-immune pathologies.[6]

TSPO in Viral Infection

TSPO and TSPO ligands were shown to modulate responses to viral infection. Apoptosis blockade is a strategy adopted by the virus to circumvent the normal protective host response against viral infection. The interaction between ML11, a virulence factor produced by the *Myxoma poxvirus*, and TSPO resulted in the inhibition of the dissipation of the transmembrane mitochondrial potential and the blockade of the mitochondrial release of cytochrome c.[31] This latter study was important as it demonstrated, for the first time, the direct interaction of TSPO with an anti-apoptotic protein. The demonstration that a pathogenic virus targets TSPO to inhibit apoptosis offers new prospects for the dissection of TSPO function but also for the definition of original anti-viral strategies.[6]

TSPO in Neurodegenerative Diseases

A dramatic increase in TSPO density has been observed following experimental injuries of the CNS and in pathological situations. In most lesions, the increase in TSPO density was associated with the inflammatory reaction of the nervous system. These conditions included inflammation,[32] metabolic stress,[33] traumatic, or ischemic chemically-induced brain injury in animal models.[34] Similar changes in TSPO density are observed in acute and chronic neurodegenerative states in humans. For example, temporal cortex obtained from patients with Alzheimer's disease show an increase in TSPO density. A highly significant increase in TSPO density was also observed in the putamen and a moderate but significant increase in the frontal cortex of patients suffering from Huntington's disease.[35] Finally, Vowinckel and co-workers observed a correlation between [^{3}H]PK11195 binding and inflammation both *in vitro* and *in vivo* in multiple sclerosis and experimental autoimmune encephalomyelitis.[36] Given these modulations, labelled PK11195 and positron emission tomography (PET) have been used for *in vivo* imaging of neuroinflammation in a variety of brain diseases and at different

disease stages to: i) detect in patients inflammatory changes and ii) monitor the progression of neuroinflammation as a marker of the disease activity. Consistent with these modulations and considering both the steroidogenic potential of TSPO ligands and the antiapoptotic property of the protein, it has been hypothesized that the modulation of TSPO functions could play neurotrophic and neuroprotective roles during neuronal damage. TSPO ligands might promote neuronal survival by acting at different levels, through the regulation of apoptosis which favoured the survival of glial cells and/or the production of mediators such as neurosteroids, cytokines or other neurotrophic factors that support nerve survival. For example in a same study the ligand SSR180575 and Ro5-4864 promoted neuronal survival and repair following axotomy.[6,37]

TSPO in Anxiety

In the brain, neurosteroids such as allopregnanolone and pregnenolone, acting as positive modulators of γ-aminobutyric type A ($GABA_A$) receptors, exerting anxiolytic activity.

Specific ligands targeting TSPO increase neurosteroid production and for this reason have been suggested to play an important role in anxiety modulation. Unlike benzodiazepines (Bzs), which represent the most common anti-anxiety drugs administered around the world, selective TSPO ligands have shown anxiolytic effects in animal models without any of the side effects associated with Bzs. Therefore, specific TSPO ligands that are able to promote neurosteroidogenesis may represent the future of therapeutic treatment of anxiety disorders. Furthermore, TSPO expression levels are altered in several different psychiatric disorders in which anxiety is the main symptom.[9]

Anxiety is a normal reaction to stress, which helps people deal with daily difficulties and cope with them. When anxiety is excessive and disabling, it may become pathological and fall under the classification of an anxiety disorder

according to the diagnostic manual definition.[38] Anxiety disorders are the most common and frequent mental disorders, affecting a significant percentage of the world's population (8-13%), and often overlapping with mood disorders and drug abuse.[39] Anxiety disorders markedly affect the living conditions of patients and their relatives, jeopardizing work and family setting. In general, anxiety disorders are treated with medication, specific types of psychotherapy, or both. Treatment choices depend on the problem and the person's preference. The diagnosis is difficult and complex because of the variety of possible causes and symptoms, often arising from highly personalized experiences. Anxiety disorders are classified as panic disorder (PD), obsessive-compulsive disorder (OCD), post-traumatic stress disorder (PTSD), generalized anxiety disorder (GAD) and social and specific phobias. A combination of pharmacological and genetic manipulation studies has provided forceful evidences that the GABAergic system is strongly linked to the development of anxiety behaviours.

The $GABA_A$ receptor is one of two ligand-gated ion channels responsible for mediating the effects of GABA, the major inhibitory neurotransmitter in the brain. In addition to the GABA binding site, the $GABA_A$ receptor complex appears to have distinct allosteric binding sites for benzodiazepines, barbiturates, ethanol, inhaled anaesthetics, furosemide, kavalactones, neuroactive steroids, and picrotoxin. The receptor is a multimeric transmembrane receptor consisting of five subunits (the most common type in the brain is a pentamer comprising two α, two β, and a γ subunit ($\alpha_2\beta_2\gamma$)), arranged around a central pore.[40] Once bound by endogenous GABA, the protein receptor changes conformation within the membrane, opening the pore to allow chloride ions to pass down the electrochemical gradient. Activation of $GABA_A$ receptors tends to stabilize the resting potential. In that condition, the excitatory neurotransmitters cannot depolarize the neuron generating the action potential, so the net effect is typically inhibitory, reducing the activity of the neuron.

The Bzs are a class of psychoactive drugs with anxiolytic, sedative, hypnotic, anticonvulsant, and muscle relaxant properties. Bzs bind at the interface of the

α and γ subunits on the $GABA_A$ receptor (BzR site). The long-term use of Bzs can cause physical dependence with risk of withdrawal symptoms and rebound syndrome. However, Bzs are the most commonly used medications to treat states of anxiety, and are ever prescribed for short term relief of severe anxiety disorders. Common medications are lorazepam, clonazepam, alprazolam, and diazepam. Once bound to the BzR, the Bz ligand locks the BzR into a conformation in which the GABA neurotransmitter has a much higher affinity for its receptor. This increases the frequency of opening of the associated chloride ion channel, thereby hyperpolarizing the membrane of the associated neuron.[9]

Neurosteroids synthesised *de novo* in the brain modulate neuronal functioning and could play an important pathophysiological role. Interestingly, a variety of neurological and psychiatric disorders, such as anxiety, depression, and schizophrenia, have been associated with both abnormal levels of neurosteroids and perturbations of neurotransmission. Some of the endogenous neurosteroid $GABA_A$ modulators are allopregnanolone (3α,5α-tetrahydroprogesterone, ALLO), pregnenolone (PREG), and tetrahydrodeoxycorticosterone (THDOC). In addition, dehydroepiandrosterone sulphate (DHEAS), the most abundant steroid found in the body, exhibits a bimodal effect on $GABA_A$ receptors: it demonstrates positive allosteric modulation at low nanomolar concentrations, and negative allosteric modulation at high micromolar concentrations. The anxiolytic properties of DHEAS may also occur since it is metabolised to androsterone and androstanediol, which are positive modulators of the $GABA_A$ receptor.

It has been recognized that neurosteroids are synthesized from cholesterol in the CNS by a cascade of enzymatic processes, controlled by both P450 and non-P450 cytochrome enzymes.[9,41] The first step in the neurosteroid synthesis is cholesterol conversion to pregnenolone, which occurs in mitochondria and is facilitated by TSPO. This step is the rate-limiting reaction of neurosteroid synthesis and appears to regulate the neurosteroid levels in the brain. The binding of TSPO ligands induces cholesterol transport and steroid formation, leading to the formation of active neurosteroids (ALLO), which positively

modulate the activity of the $GABA_A$ receptor, potentiating GABAergic transmission and thus explaining their anxiolytic activity, as primarily shown in animal models of anxiety,[41] **Figure 3.**

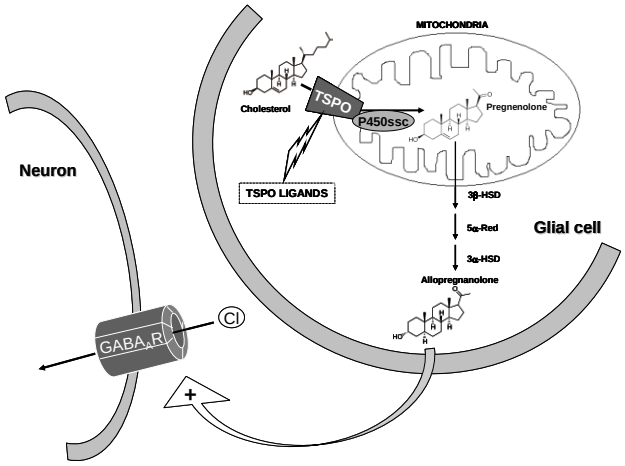

Figure 3. Role of TSPO ligands in neurosteroid-mediated allosteric modulation of the $GABA_A$ receptor (TSPO, Translocator Protein; P450ssc, Cholesterol side-chain cleavage cytochrome P-450 complex; 3β-HSD, 3β-hydroxysteroid dehydrogenase; 5α-Red, 5α-Reductase; 3α-HSD, 3α-hydroxysteroid dehydrogenase; $GABA_A$ R, $GABA_A$ receptor).

This evidence has suggested TSPO involvement in the secretion of neurosteroids, whose levels have been reported to be changed in several diseases and to be implicated in the pathogenic mechanisms of anxiety.[9,42] Indeed, the important involvement of TSPO in anxiety in humans has been extensively demonstrated by numerous studies in which TSPO expression levels have been reported to be changed. Specifically, TSPO density is up-regulated in acute stress conditions and down-regulated in chronic or repeated stress. A decrease of TSPO density has been shown in blood cells (platelets or lymphocytes) of patients affected by different psychiatric disorders, mainly characterized by anxiety, such as generalized anxiety disorder, generalized social phobia, post-traumatic stress disorder, panic disorder, chronic obsessive–compulsive disorder and also in suicidal patients,[43] as well as in healthy subjects with high trait anxiety levels. It

has been demonstrated that TSPO expression was significantly decreased in lymphocytes of patients with post-traumatic stress disorder,[44] and in platelets of patients with panic disorder or major depressive disorder associated with severe separation anxiety symptoms.[9]

TSPO Endogenous Ligands

A wide variety of endogenous molecules with affinity for the TSPO and different chemical structures have been identified.

Protoporphyrins (protoporphyrins IX, mesoporphyrins IX, deuteroporphyrins IX, hemin) exhibit a very high affinity for TSPO. As several steroidogenic tissues, such as the adrenal gland and testis, show high TSPO and porphyrin levels, it has been suggested a physiological role for the interaction of these two molecules. Furthermore, having a plane of symmetry (**Figure 4**), these molecules could bind dimerized form of TSPO, confirming in this way the postulated two-binding site model.[2,13]

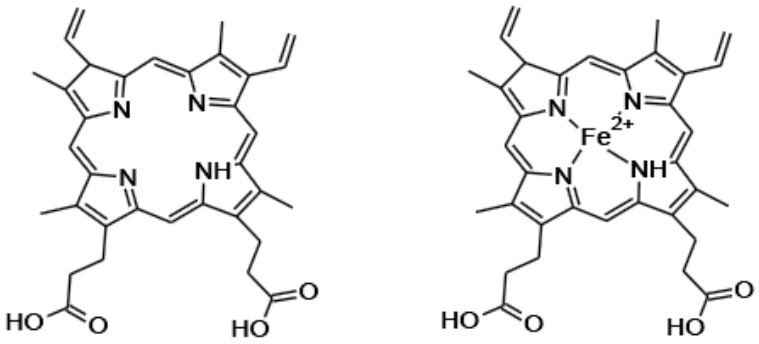

Protoporphyrin IX **Heme**

Figure 4. Chemical structures of protoporphyrin IX and heme

Another endogenous ligand is *cholesterol*, as previously reported discussing the fundamental role of TSPO in the regulation of cholesterol transport and thus in the steroidogenesis. Again it has been shown that a dimeric form of TSPO possesses an enhanced binding capacity to cholesterol.[2]

In 1984 Corda et al. isolated and purified a neuropeptide able to inhibit diazepam binding to Bz binding site on brain membranes. This 11 kDa polypeptide, named *DBI (diazepam binding inhibitor),* is constituted by 86 amino acids and binds with low affinity both TSPO and CBR, while a short fragment of DBI, triakontatetra-neuropeptide, is more selective for TSPO. Furthermore, DBI promotes loading of cholesterol to the cytochrome P-450scc and stimulates steroidogenesis by directly interacting with TSPO.[2,45]

Finally, *anthralin*, a 16 kDa protein that has been demonstrated interact with both TSPO and dihydropyridine binding site, and *phospholipase A2* have also been proposed as endogenous ligands for TSPO.[2]

TSPO Synthetic Ligands

Synthetic TSPO selective ligands have been developed with the aim to deepen the knowledge of the exact pharmacological role of TSPO, to define its involvement in several patho-physiological conditions and to establish the structural requirements needed for an optimum of affinity.

Initially, the most of these ligands have been designed starting from classical selective CBR ligands, such as benzodiazepines, making the necessary structural modifies in order to shift the affinity toward TSPO. Until to date, the prototypic ligands, used as reference compounds in the development of TSPO pharmacophore models and in SAR studies, are the benzodiazepine Ro5-4864 and the isoquinolinecarboxamide PK11195.[13]

Subsequently, a number of diversified structures have been developed obtaining in some cases good results in term of affinity and selectivity, and leading to draw various TSPO pharmacophore models useful for designing novel synthetic derivatives. TSPO specific synthetic ligands do not have a typical shared structure and thus can be distinguished nine different classes of compounds (**Figure 5**)[11]:

- Benzodiazepines (Diazepam, Ro5-4864)

- Isoquinoline and Quinazoline Carboxamides (PK11195)
- Benzothiazepines (THIA-66, THIA-67, THIA-4i)
- Benzoxazepines (Oxa-17f, Oxa-17j)
- Imidazopyridines (Alpidem)
- Phenoxyphenyl-Acetamide Derivatives (DAA1106)
- Pyrazolopyrimidines (DPA-713)
- Indolacetamide Derivatives (FGIN-1, SSR180575)
- Indol-3-ylglyoxylamides (IND-18)

Benzodiazepines

The classical Bz, Diazepam, has long been used as an anxiolytic and also as an effective anticonvulsant. Its ability to enhance the affinity of GABA for its receptor by binding to the modulatory site has been well characterized. In 1977, Braestrup and Squires performed a study concerning the binding properties of [^{3}H]Diazepam, identifying an alternative, saturable and specific binding site located on rat brain membranes and on mitochondrial fractions from rat kidney, liver and lung.[1] Starting from this discovery, Bz-binding sites have been divided into central and peripheral types. Diazepam binds with nearly similar nanomolar affinity to both receptors, but other ligands show selectivity. Actually, the clinically inactive benzodiazepine Ro5-4864 (4'-clorodiazepam), showed high affinity for this peripheral site, now TSPO, and was unable to displace [^{3}H]Diazepam from the central binding site. The main disadvantage of Ro5-4864 is its species dependence, which implied markedly different results between rats and humans, partially limiting its usefulness as a tool to study TSPO.[9]

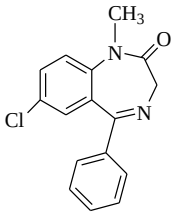

Diazepam

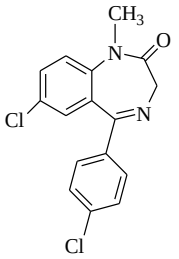

Ro 5-4864

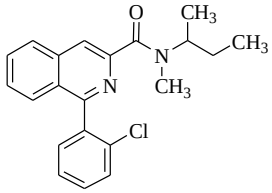

PK 11195

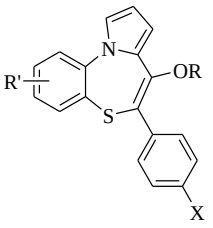

THIA-66: R=$COCH_3$, R'=H, X=OCH_3
THIA-67: R=SO_2CH_3, R'=H, X=OCH_3
THIA-4i: R=$CON(Et)_2$, R'=4-Cl, X=H

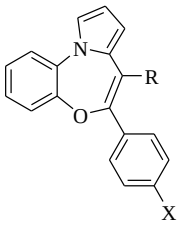

OXA-17f: R=$OCON(Et)_2$, X=H
OXA-17j: R=$OCON(Et)_2$, X=CH_3

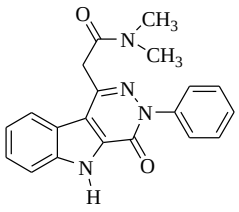

SSR 180575

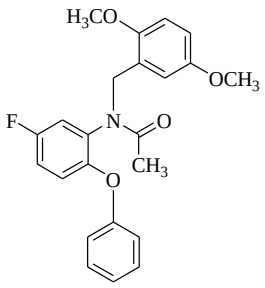

DAA 1106

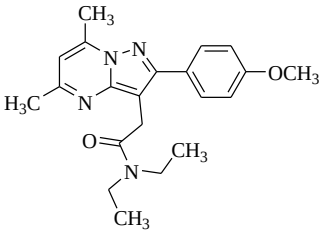

DPA 713

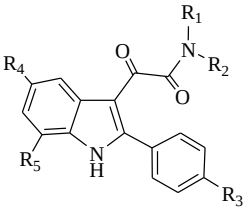

IND-18: R_1=R_2= n-C_6H_{13}, R_3=F, R_4=H

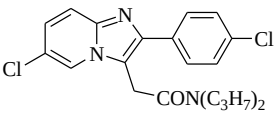

Alpidem

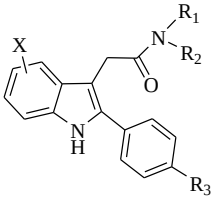

FGIN-1
FGIN-1-27: R_1=R_2= n-C_6H_{13}; R_3=F

Figure 5.

Isoquinoline and Quinazoline Carboxamides

The Isoquinoline Carboxamide PK11195, was the first non-benzodiazepine type compound identified to bind the TSPO with high potency, and it is nowadays the most commonly used standard for this receptor.

At the end of the nineties, it was (together with a number of structurally related analogues) widely used for studies aimed to define and map the binding site.

Cappelli *et al.* presented a novel systematic approach to the study of the binding of PK11195-like compounds within TSPO site based on the design of conformationally constrained derivatives (**II**-**IX**, **Figure 6**) in which the orientation of the carbonyl dipole is suitably spaced around its degree of conformational freedom.[46] Most of these derivatives showed TSPO affinities in the nanomolar range, **Table 1**. The carbonyl function was confirmed as the primary pharmacophoric element in the recognition at TSPO. Ligands with the greatest affinity (**III**-**V**, **VII**-**IX**) showed a restricted range of carbonyl orientations (comprised between 80° and 110°), suggesting the involvement of this moiety in a specific hydrogen-bonding interaction with suitable amino acids in the receptor. Quantitative structure-activity relationship (QSAR) studies evidenced that secondary amide derivatives showed significantly lowers TSPO affinity when compared with tertiary amides, and both benzyl and sec-butyl substituents raised as optimal groups for the interaction with the receptor. The pendant phenyl ring also held an essential pharmacophoric function. Finally the position and role of the nitrogen atoms in the quinoline and isoquinoline nuclei seemed to be irrelevant.

Some years after, the same research group[47] studied the radiolabelling of three quinoline derivatives (N-[^{11}C]-**III**, N-[^{11}C]-**IV**, N-[^{11}C]-**V**) aiming to develop potential tools for the non-invasive assessment of TSPO *in vivo* by means of PET, in various pathological conditions including multiple sclerosis, human glioma, cerebral infarction and calcium channel anomalies in heart diseases. From these studies *N*-[^{11}C]-**V** emerged of potential interest for *in vivo* imaging of TSPO, due to its high specific binding, as indicated by the high reduction of radioligand

uptake observed in the inhibition study with cold PK11195, and tissue-to-blood ratio. Evaluation of these ligands for *in vivo* measuring of TSPO expression in a preclinical model of Huntington's disease, indicated that *N*-[^{11}C]-**V** is a promising candidate for in vivo PET monitoring of neurodegenerative processes.

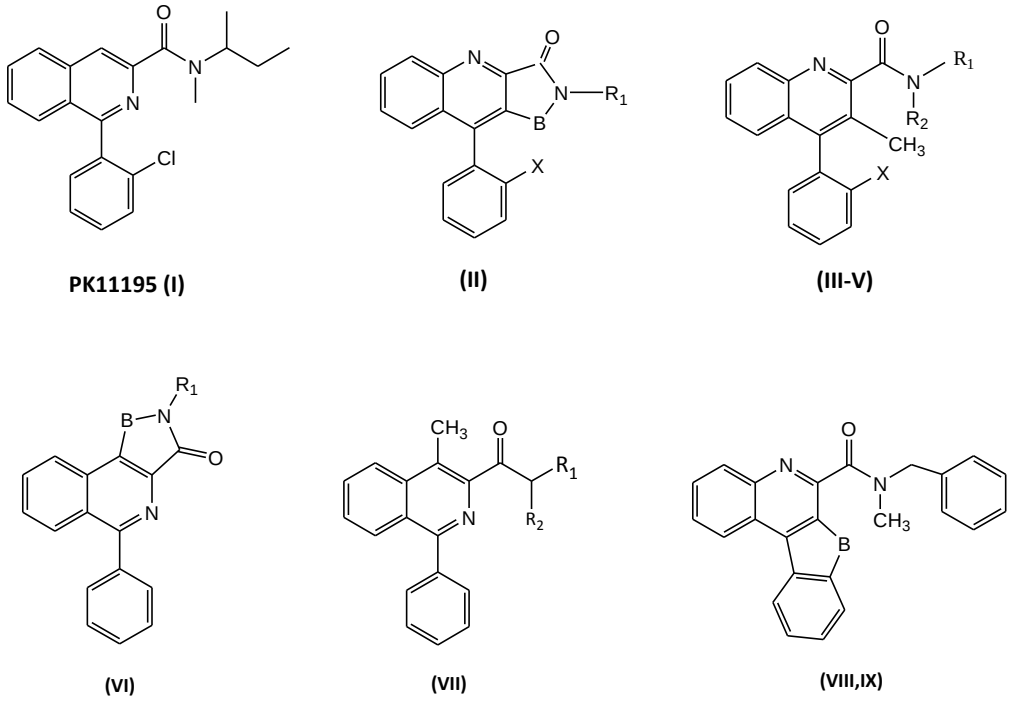

Figure 6.

Table 1. Structures and TSPO Affinities of PK11195-Like Compounds **II-IX**.

Compound	Bridge(B)	X	R_1	R_2	IC_{50}(nM)[a]
I[b]	-	-	-	-	2.2
II[b]	CH_2	H	$CH(CH_3)C_2H_5$	-	$>10^4$
III[b]	-	H	$CH(CH_3)C_2H_5$	CH_3	2.1
IV[b]	-	F	$CH(CH_3)C_2H_5$	CH_3	2.9
V[b]	-	H	$CH_2C_6H_5$	CH_3	2.1
VI[b]	CH_2	-	$CH(CH_3)C_2H_5$	-	620
VII[b]	-	-	$CH_2C_6H_5$	CH_3	3.1
VIII[b]	CH_2CH_2	-	-	-	8.9
IX[b]	OCH_2CH_2	-	-	-	10

[a]Affinities for [^{3}H]PK11195 binding inhibition to rat cortex homogenates. [b]Data taken from ref.46

Encouraged by these results, further studies among the quinolinecarboxamide derivatives were performed with the aim to optimize the interaction with TSPO and once again develop candidates for PET studies.[48] A novel series of quinoline compounds was synthesized to obtain a TSPO ligand liable to be labelled with different radionuclides and potentially useful in boron neutron capture therapy (BNCT).

Among the newly synthesized compounds, the tertiary amides bearing a chloromethyl or 2-fluorophenyl group (**XI**-**XIII**) showed subnanomolar TSPO affinity and were found to be more potent than reference compound PK11195, thus representing interesting candidates for radiolabelling and PET studies, **Table 2**. In addition, the powerful activity of compounds **XI**-**XII** in stimulating steroid biosynthesis demonstrated that these quinolinecarboxamide derivatives are able to reach and interact with TSPO *in vivo* and to stimulate the transport of cholesterol both in the brain and in peripheral tissue mitochondria.

Table 2. Structures and TSPO Affinities of Compounds **X-XIV**.

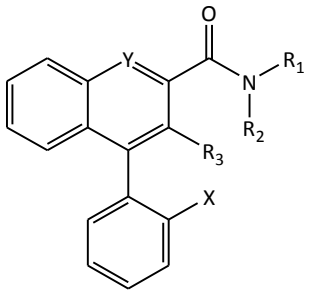

(X-XIV)

Compound	X	Y	R_1	R_2	R_3	IC_{50}(nM)[a]
X	H	N	$CH_2C_6H_5$	CH_3	CH_3	4.6
XI	F	N	$CH_2C_6H_5$	CH_3	CH_3	2.2
XII	H	N	$CH_2C_6H_5$	$CH_2C_6H_5$	CH_3	11
XIII	H	N	$CH_2C_6H_5$	CH_3	CH_2Cl	0.45
XIV	H	N	$CH_2C(B_{10}H_{10})CH$	CH_3	CH_3	73

[a]Data taken from ref. 48

As an extension of the SAR on TSPO ligands structurally related to PK11195, Anzini *et al.* performed the design of a series of carboxamide derivatives

endowed with differently substituted planar aromatic or heteroaromatic systems.[49] The main aim was to get further information on the topological requisites of the carbonyl and aromatic moieties for interaction with TSPO. New series of compounds were designed and tested (**XV**-**XIX**, **Figure 7**). Most of these derivatives showed TSPO affinity in the submicromolar range.

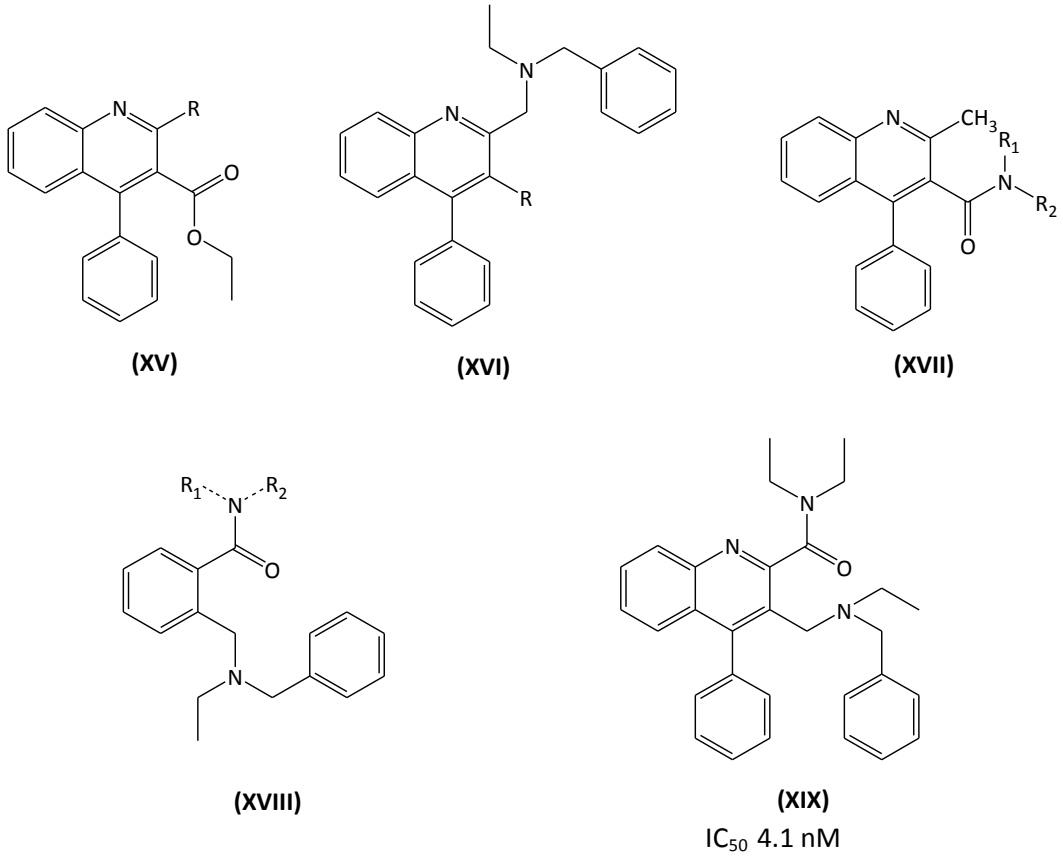

Figure 7. Structures of carboxamide derivatives (**XV**-**XIX**).

The integration of the information obtained allowed to draw the crucial structural requirements for binding with high affinity to TSPO: (i) the presence of a carbonyl dipole suitably located and oriented; (ii) lipophilic substituents attached to the 2-position; (iii) the presence of a bicyclic aromatic or heteroaromatic system bearing a suitably located pendant phenyl ring; in addition, a zone of tolerance for large substituents seems to be located in the TSPO site interacting with the 3-position of quinoline nucleus (**Figure 8**). The

most potent compound among the newly synthetized ones, **XIX**, showed a nanomolar TSPO affinity (IC_{50} 4.1 nM) similar to that shown by PK11195. Furthermore, the presence of a basic *N*-ethyl-*N*-benzylaminoethyl group in 3-position of the quinoline nucleus confers to **XIX** the possibility to make salts soluble in water. The high affinity of this compound suggested that the TSPO binding site seems to well tolerate the positive charge presumably borne by tertiary amine nitrogen at physiological pH.

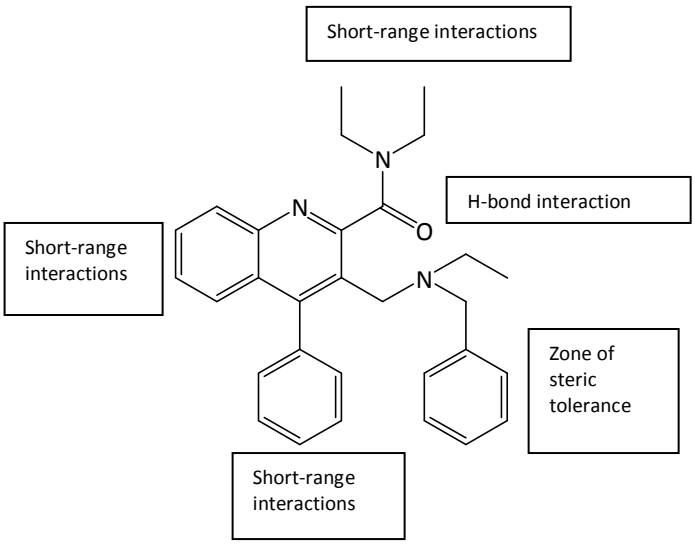

Figure 8. Schematic representation of the interaction of compound XIX with the TSPO binding site.[49]

With the aim to identify novel chemotype ligands for TSPO, a series of quinazolin-carboxamide derivatives was synthesized. Although structurally related to the isoquinolinecarboxamide PK11195, these quinazoline derivatives were assumed to have a better drug-like character, possessing a higher hydrophilicity and water solubility than their quite lipophilic isoquinoline counterpart. Indeed, preliminary calculations of several physicochemical and pharmacokinetic parameters conducted on the structures of PK11195 and of its aza-isoster supported our hypotheses. Taking into account the structural

requirements needed for high TSPO affinity and selectivity,[50] compounds featuring different combinations of R_1−R_5 substituents were designed.

Specifically, symmetrically or asymmetrically *N*,*N*-disubstituted quinazolines bearing linear, branched, or alicyclic alkyl chains were synthesized. In addition, to investigate the role of a double substitution on the amide nitrogen to gain high TSPO affinity in this class, a number of *N*-monosubstituted derivatives were studied. Finally, a chlorine atom was inserted at different positions (2', 4', 6') of the basic 4-phenylquinazoline scaffold.

All novel compounds have been tested for their affinity at TSPO in rat kidney membranes, and SARs were razionalized in light of a previously published pharmacophore/topological model of ligand−TSPO interaction (**Figure 9**),[51,52] allowing to define the main structural requirements for an optimal interaction with the target protein, that is: (i) N,N-disubstitution on the carboxamide moiety, (ii) at least one of the two N-alkyl groups with a number of carbon atoms comprised between 4 and 6. The comparison of some calculated physicochemical and pharmacokinetic properties of PK11195 and of its aza-isoster, evidenced a better drug-like character for quinazoline derivative.

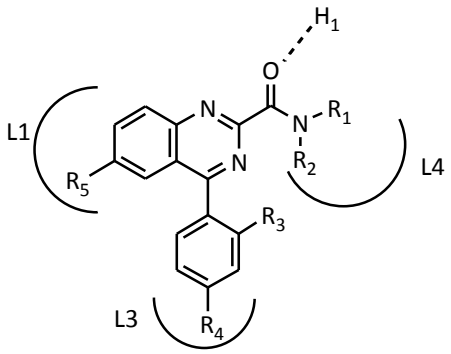

Figure 9. General structure of quinazolinecarboxamide derivatives

Benzothiazepines

The Benzothiazepines ligands, including THIA-66 and THIA-67, (**Figure 5**) displayed nanomolar affinity and notable selectivity for TSPO binding sites;

however, they were less potent than PK11195. To date, THIA-4i has been reported as the most potent TSPO ligand from this class with an affinity comparable to that of the gold standard TSPO ligand PK11195. Although these ligands might be useful probes for *in vitro* studies, further evaluation is required to elucidate their *in vivo* pharmacological profile.[11]

Benzoxazepines

The Benzoxazepines (**Figure 5**) were synthesised based on a pyrrolobenzoxazepine skeleton. Ligands from this class were evaluated in binding studies for their ability to displace [^{3}H]PK11195 from the receptor site. A number of these compounds displayed K_i values in the subnanomolar range. OXA-17f and OXA-17j were reported as the most potent TSPO ligands from this series with K_i values of 0.26 and 0.36 nM, respectively compared to K_i value of 0.78 nM for PK11195 in the same assay. All of these benzodiazepine-like compounds were shown to stimulate neurosteroids production with comparable potency to PK11195 and Ro5-4864 in mouse Y-1 adrenocortical cell line.[11]

Imidazopyrdines and Phenoxyphenyl-Acetamides

The progenitor of the class of Imidazopyridines has to be considered Alpidem (6-chloro-2-(4-chloro-phenyl)-*N*,*N*-dipropylimidazo[1,2-*α*]pyridine-3-acetamide) (**Figure 5**), known to bind both TSPO and BzR with nanomolar affinity (K_i 0.5-7 nM and 1-28 nM, respectively). Alpidem possesses anxiolytic activity with a profile that is substantially different from that of Bzs. Alpidem was released in 1991 (Ananxyl®, Sanofi-Aventis) as a highly active anxiolytic agent and it was generally prescribed to patients with moderate to severe anxiety, particularly when these patients exhibited either sensitivity or resistance to Bz therapy. Alpidem was withdrawn from the market in most of the world, following reports of severe liver damage caused by Ananxyl.[9]

In 1997, Trapani's research group reported a wide SAR study on alpidem, developing a series of 2-phenylimidazo[1,2-*a*]pyridine derivatives (CB) that showed various degrees of affinity and selectivity for TSPO with respect to BzR, dependent on the value of n and the nature of the various substituents R_1, R_2, X, Y, Z,[53] **Figure 10.**

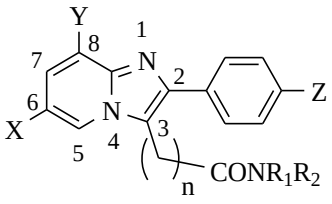

CB

Figure 10. General formula of 2-phenylimidazo[1,2-*a*]pyridine derivatives CB.

Three lead compounds selected from this series, *N*,*N*-di-*n*-propyl-[2-(4-chlorophenyl)-6,8-dichloroimidazo[1,2-*a*]pyridin-3-ylacetamide CB34, *N*,*N*-di-*n*-propyl-[2-phenyl-6,8-dichloroimidazo[1,2-*a*]pyridin-3-ylacetamide CB50, and *N*,*N*-di-*n*-propyl-[2-phenyl-6-bromo-8-methylimidazo[1,2-*a*]pyridin-3ylacetamide CB54 were investigated for their ability to stimulate central and peripheral steroidogenesis and to produce anticonflict action in rats,[54] **Figure 11.**

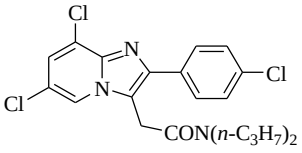

CB34

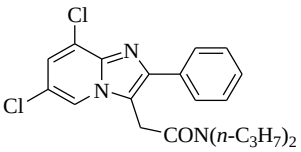

CB50

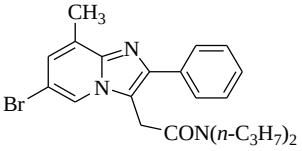

CB54

Figure 11. Imidazopyridines tested *in vivo* as anxiolytics.

In *in vitro* experiments performed on cerebral cortex membrane, all three compounds potently inhibited [^{3}H]PK11195 binding in the order CB34 (IC_{50} 1.03

nM) > CB54 (IC_{50} 1.54 nM) > CB50 (IC_{50} 3.04 nM), without substantially affecting [^{3}H]flunitrazepam binding to BzRs. Intraperitoneal administration of CB compounds in rats resulted in significant dose-dependently increased concentrations of neuroactive steroids, such as pregnenolone, progesterone, allopregnanolone, and allotetrahydrodeoxycorticosterone (THDOC) in plasma and brain. CB34 also increased the brain concentration of neuroactive steroids in adrenalectomized-orchiectomized rats, although to a lesser extent than in sham-operated animals. The effect of these ligands on neurosteroid concentration was attributable to increased steroidogenesis in the brain, rather than to an increased supply from peripheral sources. In this view, CB34 appeared to be a promising compound, which, acting as TSPO agonist, increased neuroactive steroid concentration, and proved beneficial for the treatment of stress and anxiety related diseases.[9]

In 2004, the research group of Nakazato and colleagues from the Taisho Pharmaceutical and Co. described a novel class of selective TSPO ligands derived from a structural simplification of the bicyclic structure of the benzodiazepine Ro5-4864, which is the opening of the diazepine ring. The resulting Phenoxyphenyl-Acetamide derivatives with general formulae DAA, were synthesized and evaluated for their affinity and selectivity for TSPO in an extensive SAR study,[55] **Figure 12.**

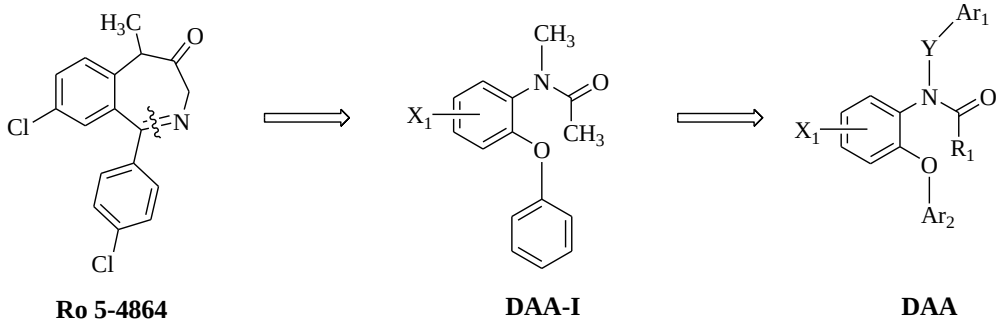

Ro 5-4864 **DAA-I** **DAA**

Figure 12. Design of DAA derivatives starting from Ro5-4864.

The Authors focused their attention on chemical modification of Ar_1, Ar_2, R_1, X_1, and Y, obtaining a number of compounds with remarkable affinity and selectivity, so that to define the most important structural features for this class of compounds in binding to TSPO.

Two phenoxyphenylacetamide derivatives, *N*-(2,5-dimethoxybenzyl)-*N*-(5-fluoro-2-phenoxyphenyl)acetamide (DAA1106) and *N*-(4-chloro-2-phenoxyphenyl)-*N*-(2-isopropoxybenzyl)acetamide (DAA1097), **Figure 13**, have been extensively characterized with respect to their receptor binding and behavioural profile, as well as to their effect on steroidogenesis.

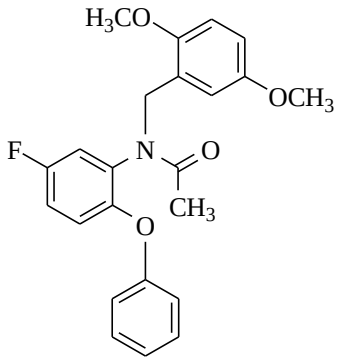

DAA 1106

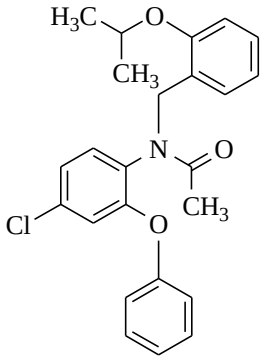

DAA 1097

Figure 13. Structure of DAA1106 and DAA1097 derivatives.

Both DAA1106 and DAA1097 inhibited [^{3}H]PK11195 and [^{3}H]Ro5-4864 binding to crude mitochondrial preparations of rat whole brain with IC_{50} values in the subnanomolar range (0.92 and 0.28 nM, and 0.64 and 0.21 nM, respectively).[56] These compounds were also highly selective, as they did not inhibit the binding of BzR ligand [^{3}H]flunitrazepam (IC_{50} > 10,000 nM) in the same preparation, and showed weak or negligible affinity (IC_{50} values are approximately 10,000 nM) for 58 other receptors, including those of related neurotransmitters, ion channels, uptake/transporter and second messengers.

In a separate study the same research group performed an exhaustive characterization of the binding of DAA1106 in the mitochondrial fractions of rat

brain by means of its [^{3}H]radiolabelled analogue. The binding of [^{3}H]DAA1106 was saturable, with a dissociation constant (K_d) determined from a Scatchard plot analysis of 1.2 nM. The binding was inhibited by several TSPO ligands in an order similar to that observed for [^{3}H]PK11195, with DAA1106 being the most potent inhibitor. In addition, [^{3}H]DAA1106 was highly TSPO selective, as its binding was not affected by several neurotransmitter-related compounds, including adrenoceptor, GABA, dopamine, 5-hydroxytriptamine (5-HT), acetylcholine, histamine, glutamate and BzR ligands even at a concentration of 10 µM. When tested on mitochondrial fractions of the rhesus monkey cerebral cortex, [^{3}H]DAA1106 showed a high affinity for TSPO (K_d 0.426 nM), with its binding being potently inhibited by DAA1106 and PK11195, but not by Ro5-4864, even at 1 µM. The results indicated that this ligand was not species dependent, similar to PK11195 and contrary to Ro5-4864. Autoradiography and biochemical studies on rat brain showed that the highest binding of [^{3}H]DAA1106 is localized in the olfactory bulb and ventricular structures related to the secretion of cerebrospinal fluid (choroid plexus), followed by the cerebellum and cerebral cortex.[9] In *in vivo* studies, DAA1106 and DAA1097 showed potent anxiolytic-like properties in laboratory animals, in both the light/dark exploration test in mice and the elevated plus-maze test in rats.[54]

Even though these two phenoxyphenylacetamides have a similar structure, potently bind to TSPO and exert anxiolytic effects, their effects on steroidogenesis appeared to be opposite. Culty and colleagues [57] examined the effects of these two ligands on steroidogenic response using MA-10 Leydig tumor cells, C6-2B glioma cells, and rat brain mitochondria. It has been observed that DAA1097 activated steroidogenesis in all the three preparations in a similar fashion to that described for PK11195, and more efficiently on brain than Leydig cells. Surprisingly, DAA1106 did not activate steroidogenesis, despite its high affinity for TSPO.

It has been suggested that the DAA1097 and DAA1106 binding sites on TSPO share a common domain with that of PK11195, but also appear to contain

additional motif(s) that do not interact efficiently with PK11195 site. The different effect on steroidogenesis has been rationalized by hypothesizing that the binding of DAA1097 induce changes in the receptor similar to that triggered by PK11195, allowing steroidogenesis activation. On the contrary, the binding of DAA1097 leads to conformational changes that do not permit or antagonize TSPO steroidogenic function.[9, 55]

Pyrazolopyrimidines

The Pyrazolopyrimidines (**Figure 5**) are bioisteres of the imidazopyridine derivatives and hence are structurally related to alpidem. Binding assays, using [^{3}H]PK11195 as the radioligand and membranes from rat kidney tissue as receptor source, showed that a subset of ligands from this pyrazolopyrimidine series displayed high binding affinity (K_i) for the TSPO ranging from 0.8-6.1 nM. Some of these compounds were shown to stimulate steroid biosynthesis in C6 glioma rat cells with a few capable of increasing pregnenolone synthesis with similar potency to Ro5-4864 and PK11195.[58]

Indoleacetamide Derivatives

The Indoleacetamide derivatives were found to enhance steroidogenesis and to be highly selective for the TSPO. The lead compound from this class is known as *N,N*-di-*n*-hexyl-2-(4-fluorophenyl)indole-3-acetamide (FGIN-1-27,[26] **Figure 5**). FGIN-1-27 has a high affinity (K_i 5.0 nM, displacement study using [^{3}H]PK11195) and is able to penetrate the blood brain barrier. FGIN-1-27 has also been shown to induce sedation and ataxia at micromolar intravenous doses. It was hypothesised that the pharmacological actions of this compound are most likely due to its indirect action on $GABA_A$ receptors *via* the stimulation of neurosteroid production.[11]

SAR studies allowed the authors to identify the structural features of FGIN-1 derivatives essential for high affinity: (i) the presence of two alkyl groups on the

amide nitrogen; (ii) the length of such alkyl chains, with the *N*,*N*-di-n-hexyl groups conferring an optimum of affinity, twenty fold higher than the corresponding *N*,*N*-dimethyl analogues; (iii) halogenation of the pendant 2-aryl groups and the indole benzofused ring (X and R_3 = Cl, F). Broad screening studies revealed that these FGIN-1 derivatives were highly TSPO selective, as they failed to bind with any significant affinity (K_i > 1000 nM) to other receptor systems, including the $GABA_A$, $GABA_B$, glycine, glutamate, dopamine, serotonin, opiate, cholecystokinin, beta adrenergic, cannabinoid, and sigma receptors. Compounds exhibiting the highest TSPO binding affinity were selected to evaluate their ability to stimulate pregnenolone formation from the mitochondria of C6-2B glioma cells.[9]

Another high affinity TSPO ligand structurally related to this class of compounds, 7-chloro-*N,N*,5-trimethyl-4-oxo-3-phenyl-3,5-dihydro-4*H*-pyridazino[4,5 *b*]indole-1-acetamide (SSR180575, **Figure 5**), has been shown to promote neuronal survival and repair. SSR180575 displays nanomolar affinity, four times greater than that of Ro5-4864, for both the rat and human TSPO. Moreover, SSR180575 increased pregnenolone accumulation in the brain implying that the therapeutic effects may be mediated through its ability to stimulate steroidogenesis.[11]

N,*N*-dialkyl-2-phenylindol-3-ylglyoxylamides

In the last decade, a novel series of highly potent and selective TSPO ligands, which represent conformationally constrained analogues of FGIN-1 derivatives, was developed and they are known as the *N*,*N*-dialkyl-2-phenylindol-3-ylglyoxylamides (**XX**, **Figure 14**).[9,59] Within this class, SAR studies were rationalized in light of the recently reported pharmacophore/receptor model made up of three lipophilic pockets (L1, L3, and L4) and an H-bond (H1) donor group, **Figure 14.**

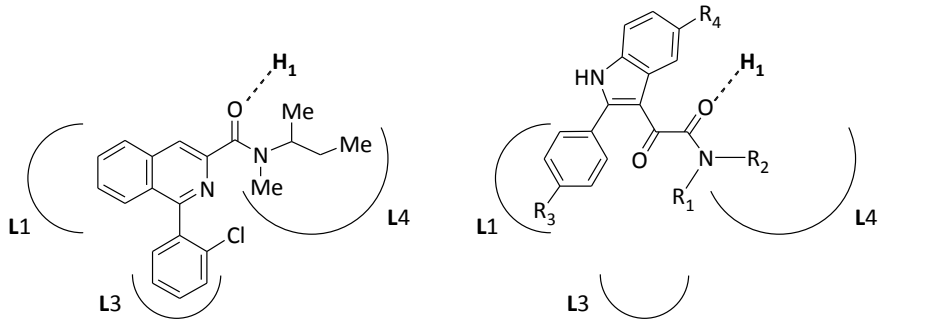

PK 11195 *N,N*-Dialkyl-2-phenylindolylglyoxylamides **XX**

Figure 14. PK11195 and *N*,*N*-dialkyl-2-phenylindolylglyoxylamides in the pharmacophore/receptor model of TSPO.

The SAR data deriving from the biological results of the newly synthesized *N*,*N*-dialkyl-2-phenylindol-3-ylglyoxylamide TSPO ligands led to a refinement of TSPO pharmacophore/topological model: (i) the R3 substituent has to be electron-withdrawing to reinforce a putative π-stacking interaction between the 2-phenyl and an electron-rich aromatic ring within the L1 pocket; (ii) R4 has to be both electronwithdrawing and very small for optimal binding, a combination of properties featured only by fluorine; (iii) substitutions in the 7-position of the indole nucleus (R5) do not produce any gain in affinity; (iv) an aromatic moiety (R1/R2) is equivalent to an aliphatic moiety of similar size in interacting hydrophobically with the L3 or L4 lipophilic pocket; (v) the L3 and L4 pockets are probably different in their dimensions, as the best-performing substitution pattern on the amide nitrogen is obtained with R1 and R2 of different sizes.

Most of the new compounds exhibited a high affinity for TSPO, with *K*i values in the nanomolar/subnanomolar range, and stimulated steroid biosynthesis in rat C6 glioma cells to an extent similar to or higher than that of classic TSPO ligands such as PK11195, Ro5-4864, and alpidem. Furthermore, in the EPM test, the indole derivative featuring R_1=CH_2CH_3, R_2=$CH_2C_6H_5$, R_3=R_4=Cl, and R_5=H, elicited an anxiolytic activity.

Taken together, the results of the present study suggest that the novel *N*,*N*-dialkyl-2-phenylindol-3-ylglyoxylamides may represent promising pharmacological tools suited for the treatment of anxiety disorders.

Molecular Probes for the receptor characterization using Chemical and Physical Techniques: Radioligands and Fluorescent Ligands

Molecular Imaging is a new discipline that unites molecular biology and *in vivo* imaging. It enables the visualization of the cellular function and the follow-up of molecular processes in living organisms without perturbing them. The multiple and numerous potentialities of this field are applicable to the diagnosis of diseases such as cancer, and neurological and cardiovascular diseases. This technique also contributes to improve the treatment of these disorders by optimizing the pre-clinical and clinical tests of new medications. It is also expected to have a major economic impact due to earlier and more precise diagnosis. Molecular and Functional Imaging has taken on a new direction since the description of the human genome.

Molecular imaging differs from traditional imaging in that probes known as biomarkers are used to help to image particular targets or pathways. Biomarkers interact chemically with their surroundings and in turn alter the image according to molecular changes occurring within the area of interest. This process is markedly different from previous methods of imaging which primarily imaged differences in qualities such as density or water content. The ability to image fine molecular changes opens up an incredible number of exciting possibilities for medical application, including early detection and treatment of disease and basic pharmaceutical development. Furthermore, molecular imaging allows quantitative tests, imparting a greater degree of objectivity to the study of these areas.

Many areas of research are being conducted in the field of molecular imaging. Much research is currently centered on detecting what is known as a predisease state or molecular states that occur before typical symptoms of a disease. Other important veins of research are the imaging of gene expression and the development of novel biomarkers.

There are many different modalities that can be used for noninvasive molecular imaging: Magnetic Resonance Imaging (MRI), Optical Imaging (Fluorescent probes and labels are an important tool for optical imaging.), Single photon emission computed tomography (SPECT), Positron Emission Tomography (PET).

The founding principles of molecular imaging can be traced back to nuclear medicine procedures over the past few decades, with other technologies (e.g., optical, MRI) being adapted for molecular imaging by developing different types of molecular probes. At the widest level, there exist two classes of probes: nonspecific and specific. Nuclear medicine plays a key role in the latter class, as the signaling portion of specifically targeted probes. Probes that use antibodies, ligands, or substrates to specifically interact with protein targets in particular cells or subcellular compartments include those used in most of the conventional radiotracer imaging methods, where the emphasis is on imaging final products of gene expression with radiolabelled substrates that interact with a protein originating from a specific gene. These interactions are based on either receptor-radioligand binding (e.g. binding of ^{11}C-carfentanil to the mu opiate receptor) or enzyme mediated trapping of a radiolabelled substrate (e.g. ^{18}F-2-fluoro-2-deoxyglucose [^{18}F-FDG] phosphorylation by hexokinase).

However, the main limitation of most of these specific approaches is that a new substrate must be discovered and radiolabelled to yield a different probe for each new protein target. With the significant difficulty, cost, and effort involved in radiolabeling new substrates, along with the requirement for in vivo characterization of every substrate under investigation, more generalizable methods (i.e. those that can image gene product targets arising from the expression of any gene of interest) are preferred. In recent years, this issue has

propelled the development and validation of molecular imaging reporter gene/reporter probe systems for use in living subjects together with other generalizable strategies.

The various existing imaging technologies differ in five main aspects: (i) spatial resolution; (ii) depth penetration; (iii) energy expended for image generation (ionizing or no ionizing, depending on which component of the electromagnetic radiation spectrum is exploited for image generation); (iv) availability of injectable/biocompatible molecular probes; and (v) the respective detection threshold of probes for a given technology, **Table 3**.

Molecular imaging has revolutionized the practice of medicine and is critical to quality health care. Molecular imaging delivers on the promise of "personalized medicine"; it can provide patient-specific information that allows treatment to be tailored to the specific biological attributes of both the disease and the patient.

With molecular imaging, abnormalities may be detected very early in the progression of a disease, often before medical problems can be detected by other diagnostic tests and even before symptoms occur. Such early detection allows a disease to be treated early when there may be a more successful outcome.

A molecular imaging probe is a molecule used in molecular imaging to deliver a tracer to a specific organ or tissue. Some examples of molecular probes are Radioligands and Fluorescent ligands.

Table 3. Key advantages and disadvantages of the main available imaging modalities used in molecular approaches.

Imaging Technique	**EM Radiation Spectrum Used In Image Generation**	**Advantages**	**Disadvantages**
Positron emission tomography (PET)	High energy gamma rays	- high sensitivity; isotopes can substitute naturally occurring atoms; - quantitative; - translational research	- PET cyclotron or generator needed; - relatively low spatial resolution; - radiation of subject
Single photon emission computed tomography (SPECT)	Lower energy gamma rays	- availability of many molecular probes; - possibility to image multiple probes simultaneously; - possibility to be adapted to clinical imaging systems	- relatively low spatial resolution; - radiation
Optical bioluminescence imaging	Visible light	- highest sensitivity; - quickness and easiness: - low cost, and relatively high throughput	- low spatial resolution; - current 2-D imaging only; - relatively surface-weighted; - limited translational research
Optical fluorescence imaging	Visible light or near-infrared	- high sensitivity; - detection of fluorochrome in live and dead cells	- relatively low spatial resolution; relatively surface-weighted
Magnetic resonance imaging (MRI)	Radio waves	- highest spatial resolution; - combines morphologic and functional imaging	- relatively low sensitivity; - long scan and postprocessing time; - mass quantity of probe may be needed
Computed tomography (CT)	X-rays	- bone and tumor imaging; - anatomic imaging	- limited 'molecular' applications; - limited soft tissue resolution; - radiation
Ultrasound	High-frequency sound	- real time; - low cost	- limited spatial resolution; - mostly morphologic although targeted microbubbles under development

PET and Radioligands

Positron emission tomography (PET) is a nuclear medicine imaging technique which produces a three-dimensional image or picture of functional processes in the body. PET uses radiopharmaceuticals that emit positrons (positively charged electrons). A radiopharmaceutical such as FDG (Fludeoxyglucose (^{18}F)), an analogue of glucose, is injected into the patient, the concentration of the tracer imaged then gives tissue metabolic activity in terms of regional glucose uptake. The fluorine emits positrons which react with the first electron they come in contact with, annihilating both and producing energy according to Einstein's famous $E=MC^2$ formula. This energy takes the form of two photons (particles of light) with a very specific energy level that shoot off in opposite directions. When these photon pairs are detected by the PET scanner, the location of the original fluorine atom can be extrapolated. Although positron/electron annihilation is one of the most powerful reactions known to science, the amount of mass involved is so small that the actual energy produced is not harmful to the patient, and the fluorine decays rapidly into harmless oxygen.

A PET scanner consists of a circular array of detectors tuned to detect photons at the specific energy level created by the positron/electron annihilation (**Figure 15**). Topographic reconstruction software assembles these signals into images that show the location and concentration of the radiopharmaceutical inside the patient. When scanning with FDG, the rapidly dividing cancer cells use a lot of glucose to fuel their growth; therefore, they show up as "hot spots" on the PET image.

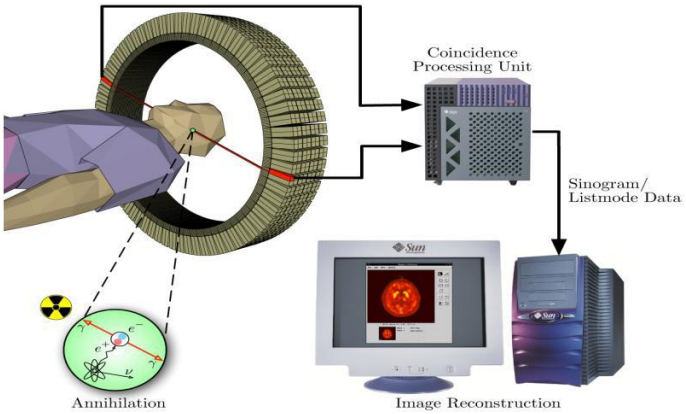

Figure 15.

PET scanning uses radionuclides, that are typically isotopes with short half lives such as carbon-11 (~20 min), nitrogen-13 (~10 min), oxygen-15 (~2 min), and fluorine-18 (~110 min). These radionuclides are incorporated either into compounds normally used by the body such as glucose (or glucose analogues), water or ammonia, or into molecules that bind to receptors or other sites of drug action. Such labeled compounds are known as radioligands.

It is important to recognize that PET technology can be used to trace the biologic pathway of any compound in living humans (and many other species as well), provided it can be radiolabelled with a PET isotope. Due to the short half lives of most radioisotopes, the radioligands must be produced using a cyclotron and radiochemistry laboratory that are in close proximity to the PET imaging facility. The half life of fluorine-18 is long enough such that fluorine-18 labeled radiotracers can be manufactured commercially at an offsite location. There is no chemical difference between the way the radioactive and non-radioactive versions of an element react. The fact that there is no difference allows the radioactive versions of the element to be substituted for the non-radioactive versions to produce a tracer.

PET is useful in diagnosing certain cardiovascular and neurological diseases as it highlights areas of increased, diminished, or absent metabolic activity. PET is mainly used in determining the presence and severity of cancers, neurological

conditions, and cardiovascular diseases. It is also used to identify and stage cancers in the initial diagnosis and to check for recurrences. An example of how PET can be uniquely useful is in following patients after radiation therapy. The radiation may create scar tissue at the cancer site. Other medical imaging techniques can only identify the scar tissue as a "mass," i.e. it looks the same before and after therapy, while PET can indicate whether or not the mass is still malignant.

PET scanning with the tracer fluorine-18 (F-18) fluorodeoxyglucose (FDG), called FDG-PET, is widely used in clinical oncology. FDG-PET can be used for diagnosis, staging, and monitoring treatment of cancers, particularly in Hodgkin's disease, non Hodgkin's lymphoma, and lung cancer. Many other types of solid tumors will be found to be very highly labeled on a case-by-case basis, a fact which becomes especially useful in searching for tumor metastasis, or for recurrence after a known highly active primary tumor is removed.

PET neuroimaging is based on an assumption that areas of high radioactivity are associated with brain activity. What is actually measured indirectly is the flow of blood to different parts of the brain, which is generally believed to be correlated with brain activity, and has been measured using the tracer oxygen-15. However, because of its 2-minute half-life O-15 must be piped directly from a medical cyclotron for such uses, and this is difficult. In practice, as the brain is normally a rapid user of glucose, and since brain pathologies such as Alzheimer's disease greatly decrease brain metabolism of both glucose and oxygen in tandem, standard FDG-PET of the brain, which measures regional glucose use, may also be successfully used to differentiate Alzheimer's disease from other dementing processes, and also to make early diagnosis of Alzheimer's disease. The main advantage of FDG-PET for these uses is its much wider availability. Several radiotracers C-11 or F-18 (i.e. radioligands) have been developed that are ligands for specific neuroreceptor subtypes of interest in biological psychiatry such as [^{11}C]-raclopride and [^{18}F]-fallypride for dopamine D_2/D_3 receptors, [^{11}C]McN 5652 and [^{11}C]DASB for serotonin transporters, or the visualization of neuroreceptor

pools in the context of a plurality of neuropsychiatric and neurologic illnesses. In addition, studies have been performed examining the state of these receptors in patients compared to healthy controls in schizophrenia, substance abuse, mood disorders and other psychiatric conditions.

PET is used also in pharmacology. In pre-clinical trials it is possible to radiolabel a new drug and inject it into animals. These scans are referred to as biodistribution studies. The uptake of the drug, the tissues in which it concentrates, and its eventual elimination, can be monitored more quickly with respect to the older technique of killing and dissecting the animals to discover the same information. Much more commonly, however, drug occupancy at a purported site of action can be inferred indirectly by competition studies between unlabeled drug and radiolabelled compounds known a priori to bind with specificity to the site. A single radioligand can be used to test many potential drug candidates for the same target. A related technique involves scanning with radioligands that compete with an endogenous (naturally occurring) substance at a given receptor to demonstrate that a drug causes the release of the natural substance.

PET imaging using specific TSPO ligands to label activated microglia may help to track the progression of neuroinflammation and may also aid in determining the effectiveness of therapies designed to treat neuroinflammatory diseases.[60] The density of TSPO is greatly increased in disease states, reflecting the inflammatory reaction to brain injury; in this vein, TSPO ligands can be used as markers of microglia activation, neuroinflammation, and neuronal damage. Radiolabelled [^{3}H]PK11195 and other TSPO ligands have been used to image neurodegenerative pathologies such as Alzheimer's disease (AD), Parkinson's disease (PD), Huntington's disease (HD), and Multiple Sclerosis (MS). PET imaging using TSPO ligands to label activated microglia and therefore neuronal cell loss can help to understand the regional brain distribution and severity of neuroinflammation and can be a valuable tool to determine different approaches to take in the treatment of each individual disease.[13]

In 1998, novel phenoxyphenyl acetamide derivatives were developed showing potent and selective binding affinities for TSPO. Among these compounds, two promising ligands, DAA1106 and DAA1197, were labeled with ^{11}C and evaluated as PET ligands for TSPO with mice, rats, and monkeys. These [^{11}C]ligands pass across the blood–brain barrier and the rat brain. Ex vivo autoradiography showed that the [^{11}C]ligands preferably distributed in the olfactory bulb and cerebellum, two regions with richer TSPO density in the rat brain. PET study determined that the [^{11}C]ligands preferably accumulate in the occipital cortex of the monkey brain, a region with a high density of TSPO in the primate brain.[61] Activation of microglia cells plays an important role in neurological diseases. PET with [^{11}C]-(R)-PK11195 has already been used to visualize activated microglia cells in neurological diseases. However, [^{11}C]-(R)-PK11195 may not possess the required sensitivity to visualize mild neuroinflammation.

In 2009 a study of Doorduin[62] evaluated the PET tracers [^{11}C]-DPA-713 and [^{18}F]-DPA-714 as agents for imaging of activated microglia in a rat model of herpes encephalitis. Uptake of [^{11}C]-DPA-713 in infected brain areas was comparable to that of [^{11}C]-(R)-PK11195, but [^{11}C]-DPA-713 showed lower non-specific binding. Non-specific uptake of [^{18}F]-DPA-714 was lower than that of [^{11}C]-(R)-PK11195. In the infected brain, total [^{18}F]-DPA-714 uptake was lower than that of [^{11}C]-(R)-PK1195, with comparable specific uptake. [^{11}C]-DPA-713 may be more suitable for visualizing mild inflammation than [^{11}C]-(R)-PK11195. In addition, the fact that [^{18}F]-DPA-714 is an agonist PET tracer opens new possibilities to evaluate different aspects of neuroinflammation. Therefore, both tracers warrant further investigation in animal models and in a clinical setting.

INTRODUCTION TO EXPERIMENTAL SECTION

Positron Emission Tomography (PET) enables evaluation of target protein expression by measuring the radioactivity of a ligand labelled with a positron-emitting radionuclide. PET studies of TSPO could offer quantitative follow-up of neuroinflammation, an advantage for biomarker-type measurement during drug development and early clinical development.[63]

[^{11}C]PK11195[64,65] was the first tracer to be consistently used in PET imaging studies of neuroinflammation, although numerous limitations have been pointed out, including a high level of non-specific binding, and a poor signal-to-noise ratios which complicate its quantification.[66] Subsequently, many groups worldwide were actively engaged in a search for TSPO ligands with improved capacities to quantify TSPO expression. Chaveau et al.[63] have recently reviewed the main TSPO ligands that have been radiolabelled, evaluated in imaging protocols, and proposed as challengers of [^{11}C]PK11195.

The first aim of this thesis work it has been the preparation of the appropriate precursor to obtain [^{18}F](*R*)-PK14105, a [^{18}F]-labelled isoquinoline derivative analogue of PK11195.

The isoquinolinecarboxamide PK14105, [*N*-methyl-*N*-(1-methyl-propyl)-1(2-fluoro-5-nitrophenyl)isoquinoline-3-carboxamide] **6** (**Figure 16**), has been previously labelled with fluorine-18 ($t_{1/2}$ – 109.7 min)[69] and evaluated in rat as a prospective radiotracer for imaging human TSPO 18 kDa with PET. This radiotracer initially appeared promising, but extensive evaluation was hindered by its rather difficult radiosynthesis based on substitution of a chloro-substituent with cyclotron–produced [^{18}F]fluoride ion (**Figure 16**).

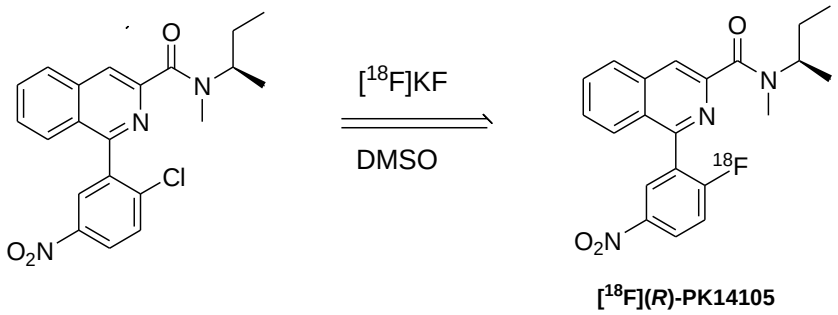

Figure 16. The synthesis of [^{18}F]PK 14105

Recently, it has been shown that simple *p*-nitroarylsulfoxides react readily with [^{18}F]fluoride ion to produce the corresponding [^{18}F]*p*-nitrofluoroarenes in good radiochemical yields.[70] This method might be applied to enhance the radiosynthesis of [^{18}F]PK14105 as its higher affinity single *R*-enantiomer, and so permit detailed evaluation of its radiotracer properties in monkey with PET. In this view, the synthesis of the sulfoxide precursor of [^{18}F]PK14105 was performed following the general synthetic route described in **Scheme 1.**

Scheme 1.

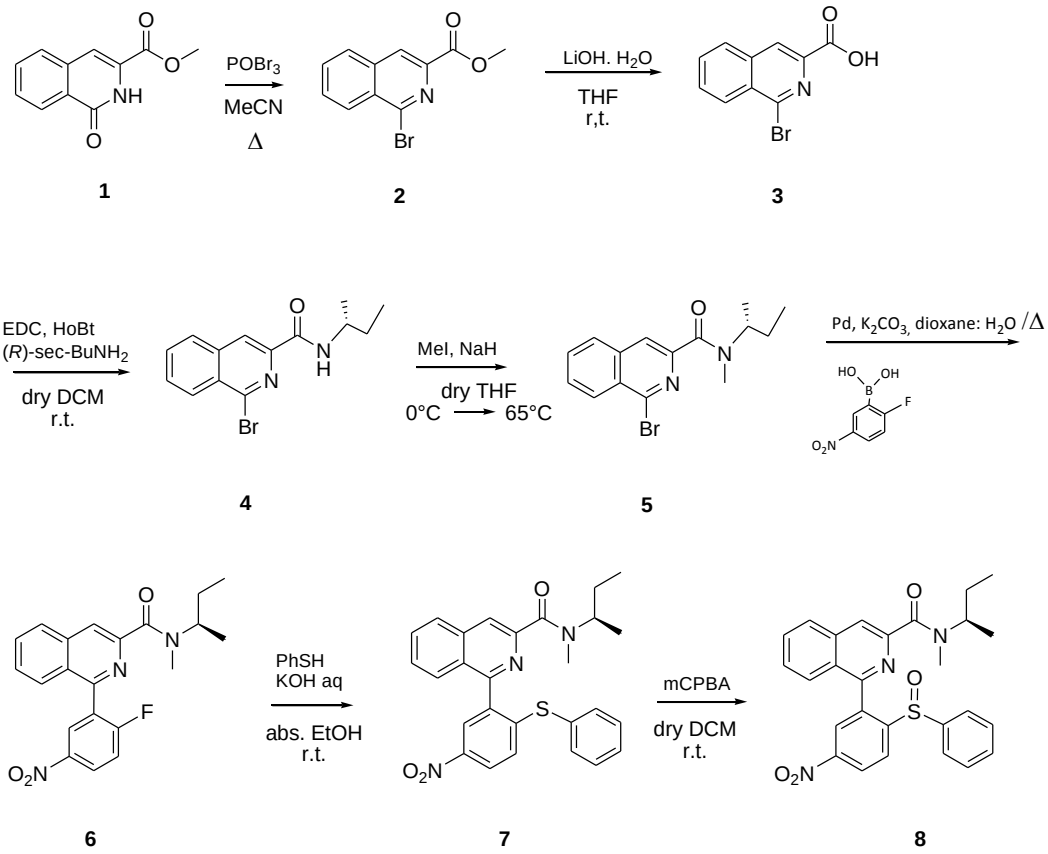

To a solution of methyl 1,2-dihydro-1-oxoisoquinoline-3-carboxylate **1** in dry acetonitrile, oxophosphobromide was added and the solution was heated to reflux for 90 minutes. The product was utilized in the following reaction without any further purification. The bromoisoquinoline ester **2** obtained was then easily hydrolyzed into the corresponding acid **3** by treatment with LiOH. To a solution of compound **3** and 1-hydroxybenzotriazole hydrate (HOBt) mixed in dry CH_2Cl_2, under nitrogen, (*R*)-*sec*-butylamine and *N*-(3-Dimethylaminopropyl)-*N*'-ethylcarbodiimide (EDC) were added and the reaction mixture was stirred at room temperature overnight. The product **4** was purified by flash chromatography (hexane:AcOEt=5:5 as eluent). Then compound **4** was methylated by treatment with sodium hydride and subsequent addition of an excess of methyl iodide to yield **5**, that was purified by flash chromatography

(hexane:AcOEt=5:5 as eluent). PK14105 (**6**) was synthesized starting from compound **5** which reacted with 2-fluoro-5-nitrophenylboronic acid using 1,1'-Bis(diphenylphosphino)ferrocene as catalyst and aqueous K_2CO_3 as base. The reaction mixture was stirred at 85 °C overnight. Product **6** was purified by flash chromatography (hexane:AcOEt=5:5 as eluent). In the next step compound **6** was dissolved in absolute ethanol and then thiophenol was added following by a solution of KOH. The reaction was mantained under stirring at room temperature until the disappearance of the starting material (TLC analysis). The sulfide **7** was then oxidated by treatment with *meta*-chloroperbenzoic acid to give the target sulfoxide **8** in 55% yield. The final product was purified by flash chromatography (hexane:AcOEt=4:6 as eluent).

The second aim of this thesis work has been to apply the same strategy to obtain a 18-F labelled derivatives featuring the quinazoline scaffold (**Figura 17**). Actually, quinazoline derivatives are assumed to have a better drug-like character with respect to the quinoline compounds, because of their higher hydrophilicity and water solubility.

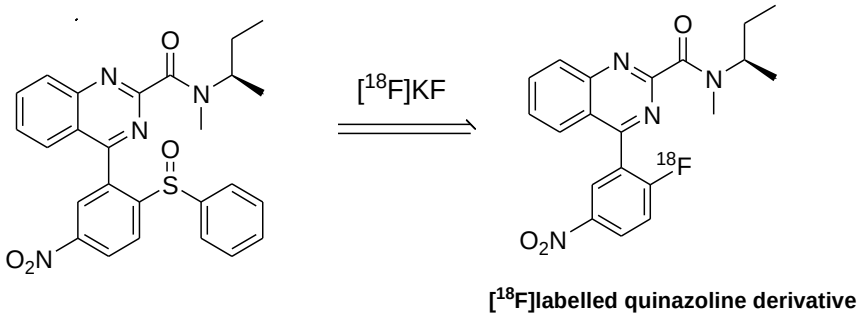

Figure 17. The planned synthesis of [^{18}F]-labelled quinazoline derivatives.

In this view, we planned to synthesize compound 16, the aza-isoster of compound **8,** following a synthetic procedure similar to that followed to obtain **8**, and outlined in **Scheme 2**.

Scheme 2.

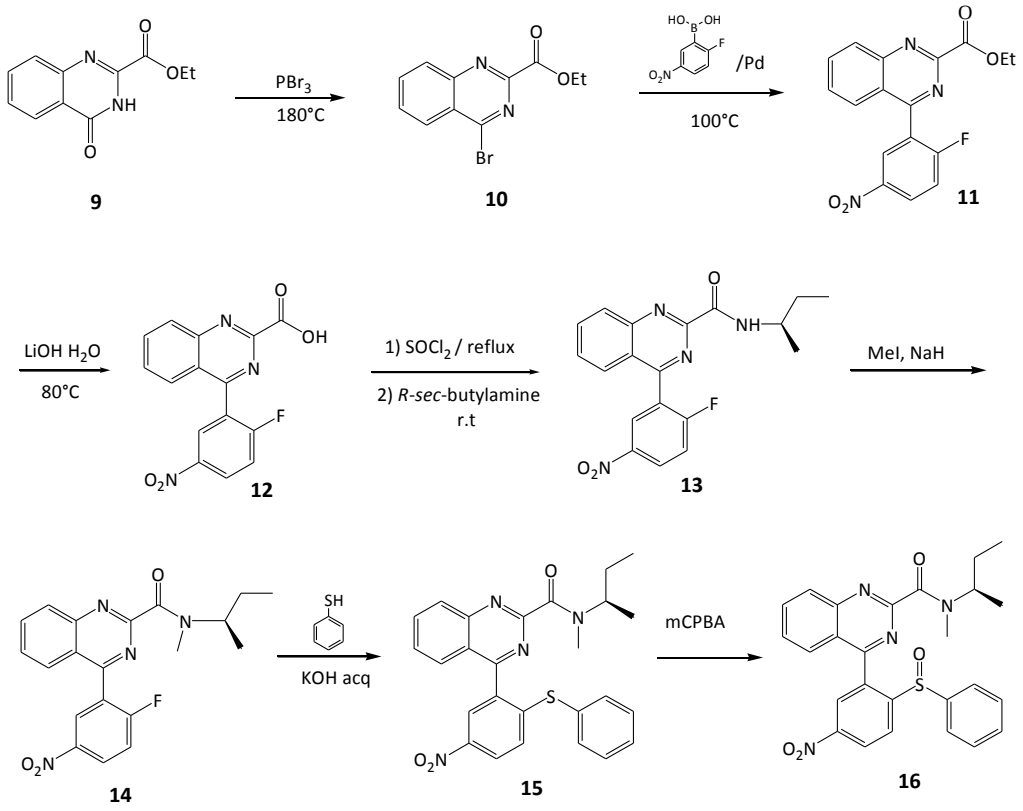

Bromination of ethyl 3,4-dihydro-4-oxoquinazoline-2-carboxylate **9** with phosphorus tribromide gave the bromoquinazoline ethyl ester **10**, that was obtained in a very low yield, about 10-12 %, because of the instability of the product. This compound was purified by flash chromatography (hexane:AcOEt=5:5 as eluent). Coupling of **10** with 2-fluoro-5-nitrophenyl boronic acid gave compound **11** in 50% yield (purification by flash chromatography: (hexane:AcOEt=6:4 as eluent). The ethyl ester moiety was easily hydrolyzed into the corresponding acid **12** and then transformed into compound **13** by reaction with $SOCl_2$, and subsequent addition of (R)-*sec*-butylamine. Also compound **13** must necessarily purified by flash

chromatography (hexane:AcOEt=6:4 as eluent) and was obtained in a very low yield (about 5%).

Because of these problems it has been tried an alternative way to prepare compound **16**, outlined in **Scheme 3**. Compound **11**, obtained as previously described, was reacted with tiophenol at room temperature overnight. Unfortunately, neither of the two products obtained and purified by flash chromatography, was the desired compound.

Scheme 3.

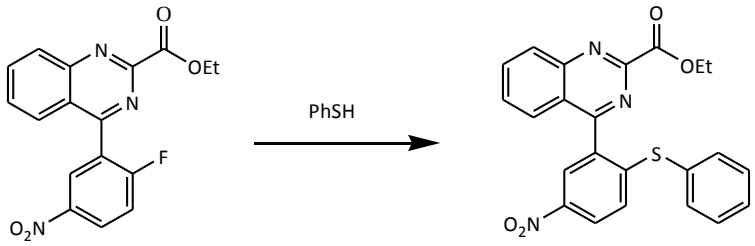

11 **17**

We are currently evaluating alternative synthetic protocols that allowed us to obtain the desired products with acceptable yields. As an example, a possible way to synthesize compound **16** is outlined in **Scheme 4**. Because of the well-known high reactivity of fluorobenzene,[71] increased also by the presence of an electron-withdrawing nitro group at the para position,[72] it should be better to react the fluoro compound with tiophenol as first step. The obtained phenyl boronic acid **19**, might be then coupled with the bromo-derivative **10**, in order to obtain compound **20.** At this point, it should be easier to prepare the amide derivative by treatment with (R)-*sec*-butylamine and also the other steps should work, too.

Scheme 4.

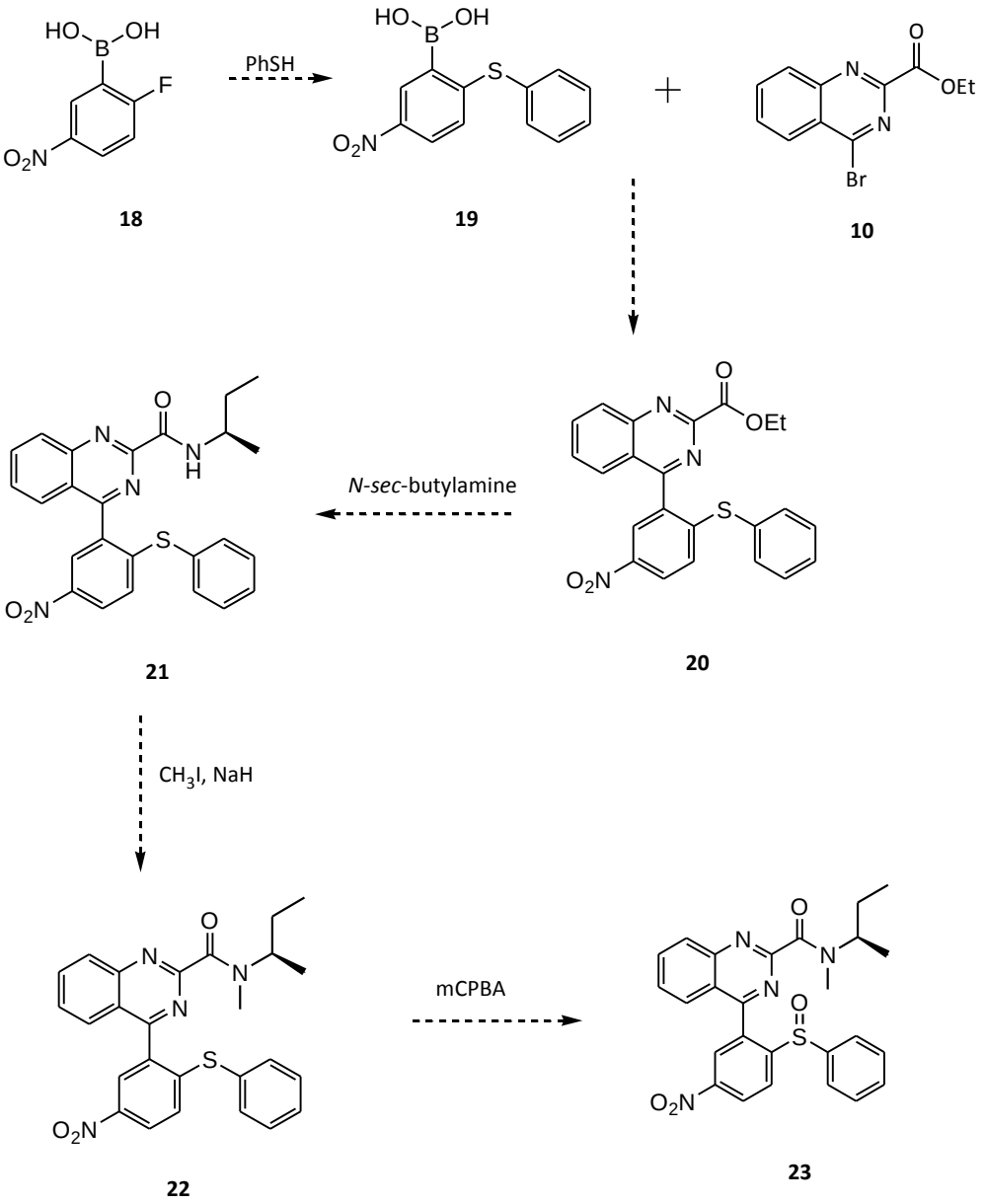
HO
B
OH
F
O2N
PhSH
S
18
19
10
OEt
Br
N-sec-butylamine
21
20
CH3I, NaH
22
mCPBA
23

Radiochemistry

Within a collaboration between the research group of Prof. Federico Da Settimo and Dr. Victor W. Pike, Senior Investigator of Molecular Imaging Branch (MIB) of the National Institute of Health (NIH), product **8** was submitted to radiolabelling reaction to obtain the desired [^{18}F]PK14105. The potential advantages of microreactor technology for PET radiochemistry are increasingly recognized.[67,68] In this study, all radiofluorination reactions were performed in a commercially available microreactor apparatus (Nanotek; Advion). The use of this apparatus offers several advantages over traditional methods of studying radiofluorination reactions, which are usually performed singly with substantial amounts of nonradioactive precursor (e.g., milligram quantities of precursor for labeling). By use of the microreactor apparatus, a series of reactions can be performed rapidly with very low fixed quantities of reagents, under precisely controlled conditions of temperature, time, and reaction stoichiometry. The whole microreactor is heated to a controlled temperature, which can be well above the boiling point of most organic solvents due to the elevated pressure of the system. **Figure 18.**

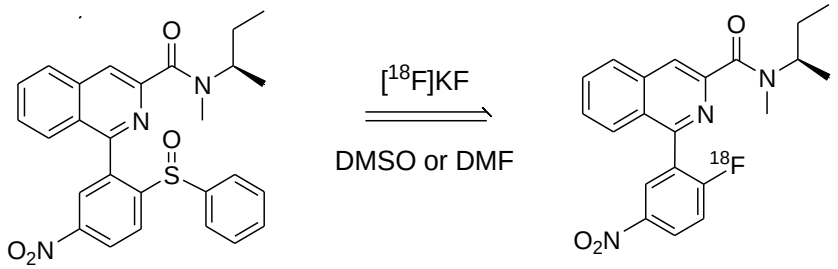

[^{18}F](*R*)-PK14105

Figure 18. Reactions of Sulphoxide with [^{18}F]Fluoride Ion

NCA (no-carrier-added) [^{18}F]-fluoride ion acqueous solution (250 ml, from a mixture of 400 ml target water and 100 ml stock solution of 0.5 mg K_2CO_3 and 5.0 mg K 2.2.2 in 9:1 MeCN and H_2O mixture) was transferred to a glass V-vial (5 ml)

that had been loaded with MeCN (600 ml), and placed in a heating well inside a lead-shielded hot-cell. Water was removed by azeotropical distillation with acetonitrile under N_2 gas flow (200 ml/min) at 110 °C. The addition of MeCN (650 ml) and heating cycle were repeated three more times. The anhydrous NCA [^{18}F]-fluoride ion-K^+ -K 2.2.2 reagent was redissolved in DMF (450 ml). This solution was then loaded into storage loop 3 of the microfluidic apparatus. A solution of precursor in anhydrous DMF (10 mM, 275 ml) was loaded into storage loop 1. A quantity of each solution (20 ml) was infused simultaneously at 4 or 2 ml/min into the 4 m-length coiled silica glass tube micro-reactor (31.4 ml) held at a set temperature. The affluent from the micro-reactor was quenched with H_2O-MeCN (1:1 v/v, 0.5 mL) and analyzed with radio-HPLC.

Table 4. Radiosynthesis of [^{18}F]PK14105 in micro-reactor

Run	**Temp (°C)**	**Flow rate (ml/min)**	**Recovery (%)**	**RCY (%) By HPLC peak**
1	**100**	**4+4**	**21**	**11.4**
2	**130**	**4+4**	**37**	**46.1**
3	**160**	**4+4**	**51**	**56.9**
4	**190**	**4+4**	**54**	**45.9**
5	**130**	**2+2**	**47**	**56.6**

The optimum temperature for the reaction in DMF was found between 130 and 160 °C and this allowed us to obtain up to 57 % of incorporation of radioactivity in our ligand.

[^{18}F](*R*)-PK14105 will now be characterized with PET as a TSPO 18 kDa radiotracer in monkey.

EXPERIMENTAL SECTION

Materials and Methods

Routine nuclear magnetic resonance spectra were recorded in DMSO-d_6 or $CDCl_3$-d_6 solution on a Bruker operating at 400 MHz. Evaporation was performed in vacuo (rotary evaporator). Analytical TLC was carried out on Merck 0.2 mm precoated silica gel aluminum sheets (60 F-254). Silica gel 60 (230-400 mesh) was used for column chromatography. Elemental analyses were performed by our analytical laboratory and agreed with theoretical values to within ±0.4%.

Methyl 4-bromonaphthalene-2-carboxylate 2. Methyl 1,2-dihydro-1-oxoisoquinoline-3-carboxylate (0.5 mmol), potassium carbonate (2.0 mmol) and Phosphorus(V) oxybromide (1.9 mmol) were heated to reflux in dry aceto nitrile (10 ml). The reaction went to completion in 90 minutes. The resulting suspension was cooled to room temperature and then concentrated to dryness. The residue was cautiously dispersed in water and the insoluble material was filtered off, washed with water and dried. The product was utilized in the following reaction without any further purification.

Yield: 61%; ^{1}H-NMR ($CDCl_3$-d_6, ppm): 3.88 (s, 3H, OCH_3); 7.93-7.84 (m, 3H, ArH); 8.36 (s, 1H, ArH); 8.47 (d, 1H, *J* = 8.0 Hz, ArH).

1-bromoisoquinoline-3-carboxylic acid 3. A solution of LiOH (13 mmol) in 10 ml of water was added to a stirred one of **2** (5 mmol) in 10 ml of anhydrous THF, and the mixture was allowed under stirring at room temperature for 60 minutes (TLC analysis). Then the mixture was acidified with HCl 6 N to pH=0 and the white precipitate was filtered off. The water was then extracted with CH_2Cl_2 and the resulting organic layer was dried over $MgSO_4$. The combinated white precipitates were dried overnight.

Yield: 85 %

***N*-*sec*-butyl-1-bromoisoquinoline-3-carboxamide 4.** Compound **3** (4 mmol) and 1-Hydroxybenzotriazole hydrate (HOBt) (6 mmol) were mixed in a round bottom flask, under nitrogen, in dry CH_2Cl_2. Then, (*R*)-(−)-*sec*-Butylamine (12 mmol) and *N*-(3-Dimethylaminopropyl)-*N*'-ethylcarbodiimide hydrochloride (EDC)(12 mmol) were added and the reaction was stirred at room temperature overnight. Organic phase was washed twice with 10 % solution of $NaHCO_3$, dried over $MgSO_4$ and then evaporated. The product was finally purified by flash chromatography (hexane:AcOEt=1:1).

Yield: 68 %; ^{1}H-NMR ($CDCl_3$-d_6, ppm): 1.00 (t, 3H, *J* = 8.0 Hz, CH_3); 1.31 (d, 3H, *J* = 4.1 Hz, CH_3); 1.68-1.63 (m, 2H, CH_2); 4.19-4.15 (m, 1H, CH); 7.83-7.76 (m, 3H, ArH); 7.98 (d, 1H, ArH, *J* = 8.0 Hz,); 8.35 (d, 1H, ArH, *J* = 8.1 Hz).

***N*-*sec*-butyl-1-bromo-N-methylisoquinoline-3-carboxamide 5.** Sodium hydride (5.4 mmol) was added portionwise, under a nitrogen atmosphere, to an ice-cooled solution of compound **4** in dry THF. After 30 minutes CH_3I was added and the solution was stirred at 65 °C overnight. The solvent was eliminated under vacuum and the residue was diluited with water and extracted with AcOEt. The product was finally purified by flash chromatography (hexane:AcOEt=1:1).

Yield: 70 %; ^{1}H-NMR ($CDCl_3$-d_6, ppm): 1.01- 0.85 (2t, 3H, *J* = 4.1 Hz, *J* = 6.2 Hz, CH_3); 1.31-1.24 (m, 3H, CH_3), 1.70-1.58 1.48-1.42 (2m, 3H, CH_3); 2.97, 2.91 (2s, 3H, CH_3); 4.79-4.75, 3.89-3.84 (2m, 1H, CH); 7.81-7.73 (m, 2H, ArH); 7.88 (d, 1H, *J* = 8.1 Hz, ArH); 7.98 (d, 1H, *J* = 8.0 Hz, ArH); 8.32 (d, 1H, *J* = 8.1 Hz, ArH).

***N*-*sec*-butyl-1-(5-fluoro-2-nitrophenyl)-*N*-methylisoquinoline-3-carboxamide 6.** Compound **5** (10 mmol), 2-Fluoro-4-Nitro-boronic acid (25 mmol), cesium carbonate (25 mmol) and 1,1'-Bis(diphenylphosphino)ferrocene (1 mmol) were combinated in a round bottom flask under nitrogen atmosphere. Then 10 ml of degassed 2:1 dioxane: H_2O were added and the reaction was stirred at 85 °C overnight. The solution was diluited with water, extracted with AcOEt, washed with brine, dried over MgSO4 and evaporated. The product was finally purified by flash chromatography (hexane:AcOEt=1:1).

Yield: 65 %; ^{1}H-NMR ($CDCl_3$-d_6, ppm): 1.00, 0.81 (2t, 3H, *J* = 6.1 Hz, *J* = 8.0 *Hz*, CH_3); 1.34-1.24 (m, 3H, CH_3); 1.72-1.59, 1.49-1.39 (2m, 2H, CH_2); 3.00-2.82 (2s, 3H, CH_3); 4.86- 4.77, 3.93-3.84 (2m, 1H, CH); 7.42 (t, 1H, *J* = 10.0 Hz, ArH); 7.68-7.63 (m, 1H, ArH); 7.81-7.73 (m, 2H, ArH); 8.04 (d, 1H, *J* = 8.1 Hz, ArH); 8.10 (d, 1H, *J* = 12.0 Hz, ArH); 8.45-8.32 (m, 1H, ArH); 8.53-8.50 (m, 1H, ArH).

***N*-*sec*-butyl-1-(5-fluoro-2-(phenylthio)phenyl)-*N*-methylisoquinoline-3-carboxamide 7.** Compound **6** (0.46 mmol) was suspended in 18 ml of absolute ethanol. Then tiophenol (0.46 mmol) was added, following by KOH (0.7 mmol) in 30 μl of water. The reaction was manteined under stirring at room temperature until the disappearance of the starting material (TLC analysis). The solvent was eliminated under vacuum and the residue was dissolved in AcOEt, washed with water, dried over $MgSO_4$ and then concentrated to dryness. The product was finally purified by flash chromatography (hexane:AcOEt=4:6).

Yield: 70 %; ^{1}H-NMR ($CDCl_3$-d_6, ppm): 1.01, 0.80 (2t, 3H, *J* = 8 Hz, *J* = 6.0 Hz, CH_3); 1.30-1.24 (m, 3H, CH_3); 1.68-1.58, 1.45-1.40 (2m, 2H, CH_2); 3.00-2.94 (2s, 3H, CH_3); 4.84- 4.80, 3.99-3.96 (2m, 1H, CH); 7.13-7.05 (m, 1H, ArH); 7.44-7.38 (m, 5H, ArH); 7.66-7.62 (m, 1H, ArH); 7.78-7.72 (m, 1H, ArH); 7.83-7.79 (m, 1H, ArH); 8.00 (d, 1H, *J* = 8.0 Hz, ArH); 8.07 (s, 1H, ArH); 8.14-8.11 (m, 1H, ArH); 8.23-8.20 (m, 1H, ArH) .

N*-*sec*-butyl-1-(5-fluoro-2-(phenylsulfinyl)phenyl)-*N*-methylisoquinoline-3 carboxamide 8.** *meta*-Chloroperoxybenzoic acid (0.15 mmol) was added to a solution of compound ***7 in 5 ml of CH_2Cl_2. The reaction mixture was stirred for 2 hours. Then, saturated acqueous solution of Na_2SO_3 was added and the organic phase was separated and washed with saturated acqueous solution of $NaHCO_3$. The combinated organic phase was dried over $MgSO_4$ and concentrated to dryness. The product was finally purified by flash chromatography (hexane:AcOEt=4:6)

Yield: 55%; ^{1}H-NMR ($CDCl_3$-d_6, ppm): 0.99-0.96, 0.80-0.73 (2m, 3H, CH_3); 1.23-1.16, 1.11 (m, d, *J* = 8.0 Hz, 3H, CH_3); 1.64-1.53, 1.46-1.39 (2m, 2H, CH_2); 2.99-2.85 (s, d, *J* = 8.0 Hz, 3H, CH_3); 4.81- 4.78, 3.95-3.68 (2m, 1H, CH) 7.15-7.07 (m, 4H, ArH); 7.31-7.23 (m, 1H, ArH); 7.49-7.45 (m, 1H, ArH); 7.75-7.70 (m, 1H, ArH);

7.97-7.92 (m, 1H, ArH); 8.10-8.04 (m, 1H, ArH); 8.32-8.29 (m, 1H, ArH); 8.56-8.42 (m, 1H, ArH).

Ethyl 4-bromoquinazoline-2-carboxylate 10. Compound ethyl 3,4-dihydro-4-oxoquinazoline-2-carboxylate (2.3 mmol) and phosphorus tribromide (46 mmol) were placed in a round bottom flask to reflux at 180°C for 2-3 hours. The solution was poured into ice, alkalinized with NH_4OH until pH=8-9, extracted with AcOEt, dried over $MgSO_4$, filtered and then evaporated to dryness. Crude compound was purified with flash chromatography (hexane:AcOEt=5:5) to give the desired product.

Yield: 10-15%. ^{1}H-NMR ($CDCl_3$-d_6, ppm): 1.52 (t, 3H, CH_3, *J*= 7,2 Hz); 4.63 (q, 2H, CH_2, *J*=10,2 Hz); 7.91-7.87 (m, 1H, ArH); 8.10-8.06 (m, 1H, ArH); 8.34-8.38 (m, 2H, ArH).

Ethyl 4-(2-fluoro-5-nitrophenyl)quinazoline-2-carboxilate 11. Compound **10** (1.1 mmol), (triphenylphosphine) Palladium (Tetrakis) (0.056 mmol) and potassium carbonate (2.2 mmol) were solubilized in anydrous toluene in a round bottom flask, under nitrogen. Then, 2-fluoro-5-nitrophenyl boronic acid (2.2 mmol) solubilized in 1 ml of absolute ethanol was added dropwise; the solution was heated at 100°C overnight. Solvents were eliminated under vacuum and the residue was dissolved in CH_2Cl_2, washed with water, dried over $MgSO_4$, filtered and then concentrated to dryness. The product was finally purified by flash chromatography (hexane:AcOEt=6:4).

Yield: 50%. ^{1}H-NMR ($CDCl_3$-d_6, ppm): 1.52 (t, 3H, CH_3, *J*= 7,2 Hz); 4.66 (q, 2H, CH_2, *J*=10,2 Hz); 7.48 (t, 1H, ArH, *J*=8,8 Hz); 7.83-7.81 (m, 2H, ArH); 8.12-8.08 (m, 1H, ArH); 8.43 (d, 1H, ArH, *J*=8,4 Hz); 8.54-8.50 (m, 1H, ArH); 8.65-8.63 (m, 1H, ArH).

4-(2-fluoro-5-nitrophenyl)quinazoline-2-carboxylic acid 12. To a solution of compound **11** (0.35 mmol) in a mixture MeOH/H2O 3:1, LiOH H_2O (0.21 mmol) was added at 0°C. The solution was manteined under stirring at 80°C overnight.
The solution was concentrated to dryness, the residue was solubilized in water and extracted in AcOEt. Water was acidified until pH=1 with HCl 10% then extracted with AcOEt, dried over $MgSO_4$, filtered and at last concentrated to dryness.
Yield= 68%.

***N-sec*-butyl-4-(2-fluoro-5-nitrophenyl)quinazoline-2-carboxamide 13.** A solution of **12** (0.24 mmol) in thionyl chloride (1.8 ml) was refluxed for 2 hours under nitrogen atmosphere. After cooling at room temperature, the excess thionyl chloride was removed at reduced pressure and the crude material dried under vacuum. To the residue, dissolved in dry THF (2ml) and cooled to 0 °C, a mixture of the (R)-*sec*-butylamine (0.24 mmol) and triethylamine (0.24 mmol) in dry THF (1.2 ml) was added dropwise. The mixture was stirred at room temperature for 48 h, filtered, and evaporated. The crude residue was dissolved in CH_2Cl_2, washed with HCl 10%, saturated NaHCO3, and water, dried, and concentrated in vacuum. Purification by column chromatography on silica gel (hexane:AcOEt=5:5).[73]
Yield=5%. ^{1}H-NMR ($CDCl_3$-d_6, ppm): 0.99 (t, 3H, CH_3, *J*= 7,4 Hz); 1.30 (d, 3H, CH_3, *J*=6,4 Hz); 1.68-1.63 (m, 2H, CH2); 4.27-4.20 (m, 1H, CH); 7.17 (d, 1H, ArH *J*= 9,2 Hz); 7.69-7.64 (m, 2H, ArH); 8.00-7.95 (m, 1H, ArH); 8.06 (bd, exch. with D_2O, 1H, NH); 8.33 (d, 1H, ArH *J*=14 Hz); 8.38 (d, 1H, *J*=2,8 Hz); 8.48-8.46 (dd, 1H, ArH *J*=2,8 Hz, *J*=2,8 Hz).

Ethyl 4-(5-nitro-2-(phenylthio)phenyl)quinazoline-2-carboxylate 17. Compound **10** (0.12 mmol) was suspended in 8 ml of absolute ethanol. Then tiophenol (0.12 mmol) was added, following by KOH (0.1 mmol). The reaction was manteined

under stirring at room temperature until the disappearance of the starting material (TLC analysis). The solvent was eliminated under vacuum and the residue was dissolved in AcOEt, washed with water, dried over $MgSO_4$ and then concentrated to dryness. The product was finally purified by flash chromatography (hexane:AcOEt=4:6). Two different products were obtained but neither of them was the desired compound.

REFERENCES

1. Braestrup, C.; Squires, R.F.. *Proc. Natl. Acad. Sci. U.S.A*. **1977**, 74, 3805-3809.

2. Gavish, M.; Bachman, I.; Shoukrun, R.; Katz, Y.; Veenman, L.; Weisinger, G.; Weizman. *Pharmacol. Rev.* **1999**, *51*, 619-640.

3. Costa , E.; Guidotti, A.; *Annu. Rev. Pharmacol. Toxicol. **1979**, 19.* 531-545

4. Papadopoulos, V.; Baraldi, M.; Guilarte, T.R.; Knudsen, T.B.; Lacapère, J.; Lindemann, P.; Norenberg, M.D.; Nutt, D.; Weizman, A.; Zhang, M.-R.; Gavish, M. *Trends Pharmacol. Sci.* **2006**, *27*, 402-409.

5. Antkiewicz-Michaluk, L.; Guidotti, A.; Krueger, K.E. *Mol. Pharmacol.* **1988**, *34*, 272-8.

6. Galiegue, S.; Tinel, N.; Casellas, P. *Curr. Med. Chem*. **2003**, *10*, 1563-1572.

7. Li, H.; Degenhardt, B.; Teper, G.; Papadopoulos, V. *Proc. Natl. Acad. Sci. USA* **2001**, *98*, 1267-1272.

8. Li, H.; Degenhardt, B.; Todin, D.; Yao, Z.X.; Tasken, K.; Papadopoulos, V. *Mol. Endocrinol*. **2001**, *15*, 2211-2228.

9. Taliani, S.; Da Settimo, F.; Da Pozzo, E.; Chelli, B.; Martini, C. *Curr. Med. Chem.* **2009**, *16*, 3359-80.

10. Casellas, P.; Galiegue, S.; Basile, A.S. *Neurochem. Int.* **2002**, *40*, 475-86

11. James, M.L.; Selleri, S.; Kassiou, M., *Curr. Med. Chem.* **2006**, *13*, 1991-2001.

12. Lacapere, J.J.; Papadopoulos, V. *Steroids* **2003**, *68*, 569–585.

13. Scarf, A. M.; Ittner, L.M.; Kassiou, M. *J. Med. Chem*. **2009**, *52*, 581-592.

14. Jamin, N.; Neumann, J.M.; Ostuni, M. A.; Vu, T.K.N.; Yao, Z.X.; Murail, S.; Robert, J.-C.;Giatzakis, C.; Papadopoulos, V.; Lacapere, J.J. *Mol. Endocrinol.* **2005**, 19, 588–594.

15. Veenman, L.; Papadopoulos, V.; Gavish, M. *Curr. Pharm. Des.* **2007**, *13*, 2385–2405.

16. Papadopoulos, V.; Lecanu, L.; Brown, R.C.; Han, Z.; Yao, Z.X. *Neuroscience* **2006**, *138*, 449-756.

17. Li, W.; Hardwick, M.J.; Rosenthal, D.; Culty, M.; Papadopoulos, V. *Biochem. Pharmacol.* **2007**, *73*, 491–503

18. Hirsch, T.; Decaudin, D.; Susin, S.A.; Marchetti, P.; Larochette, N.; Resche-Rigon, M.; Kroemer, G. *Exp. Cell Res.* **1998**, *241*, 426–434.

19. Versijpt, J.; Dumont, F.; Van Laere, K.; Decoo, D.; Santens, P.; Audenaert, K.; Achten, E.; Slegers, G.; Dierckx, R.; Korf, J. *Eur. Neurol.* **2003**, *50*, 39–47.

20. Chen, M.K.; Guilarte, R. T. *Pharmacol. Ther*. **2008**, *118*, 1-17.

21. Papadopoulos, V.; Lecanu, L. *Exp. Neurol.* **2009**, *219*, 53-57.

22. Chauveau, F.; Boutin, H.; Van Camp, N.; Dollé, F.; Tavitian, B*. Eur. J. Nucl. Med. Mol. Imaging.* **2008**, *35*, 2304-2319.

23. Pini, S.; Martini, C.; Abelli, M.; Muti, M.; Gesi, C.; Montali, M.; Chelli, B.; Lucacchini, A.; Cassano, G.B. *Psychopharmacology* **2005**, *181*, 407-11.

24. Chelli, B.; Pini, S.; Abelli, M.; Cardini, A.; Lari, L.; Muti M.; Gesi, C.; Cassano, G.B.; Lucacchini, A.; Martini, C. *Eur. Neuropsychopharmacol.* **2008**, *18*, 249-254.

25. Hardwick, M.; Rone, J.; Han, Z.; Haddad, B.; Papadopoulos, V. *Int. J. Cancer* **2001**, *94*, 322-327.

26. Kozikowski, A.P.; Ma, D.; Brewer, J.; Sun, S.; Costa, E.; Romeo, E.; Guidotti, A. *J. Med. Chem.* **1993**, *36*, 2908-20.

27. Lacor, P.; Gandolfo, P.; Tonon, M. C.; Brault, E.; Dalibert, I.; Schumacher, M.; Benavides, J.; Ferzaz, B. *Brain Res.* **1999**. *815*, 70-80.

28. Schreiber, A.A.; Frei, K.; Lichtensteiger, W.; Schlumpf, M. *Agent Actions* **1993**, *38*, 265-272.

29. Torres, S.R.; Frode, T.S.; Nardi, G.M.; Vita, N.; Reeb, R.; Ferrara, P.; Ribeiro-do-Valle, R.M.; Farges, R.C. *Eur. J. Pharmacol*. **2000**, *408*, 199-211.

30. Bribes, E.; Galiegue, S.; Bourric, B.; Casellas, P. *Immunol. Lett.,* **2003**, 2, *85*, 13-18.

31. Everett, H.; Barry, M.; Sun, X.; Lee, S.F.; Frantz, C.; Berthiaume, L.G.; McFadden, G.; Bleackly, R.C. *J. Exp. Med.* **2002**, *196*,1127-1139.

32. Banati, R.B.; Myers, R.; Kreutzbcrg, G.W. *Journal of Neurocytology* **1997**, *26*, 77-82.

33. Desjardins, P.; Butterworth, R.F. *Neurochem Int.* **2002**, *41*, 109-114.

34. Kuhlmann, A.C.; Guilarte, T.R. *J. Neurochem,* **2000**, *74*, 1694-1704.

35. Messmer, K.; Reynolds, G.P. *Neuroscience Letters* **1998**, *241*, 53-56.

36. Vowinckel, E.; Reutens, D.; Becher, B.; Verge, G.; Evans, A.; Owens, T. Antel, J.P. *J. Neurosci. Res*. **1997**, *50*, 345-353.

37. Ferzaz, B.; Brault, E.; Bourliaud, G.; Robert, J.P.; Poughon, G.; Claustre, Y.; Marguet, F.; Liere, P.; Shumacher, M.; Nowicki, J.P.; Fournier, J.; Marabout, B.; Sevrin, M.; Pascal, G.; Soubrie, P.; Benavides, J.; Scatton, B. *J. Pharmacol. Exp. Ther,* **2002**, *301*, 1067-1078.

38. DSM-IV-TR (Diagnostic and Statistical Manual of Mental Disorders, Fourth Edition - Text revision), APA Press, Washington DC. **2000**

39. National Institute of Mental Health, retrieved October 27, **2008**

40. Da Settimo, F.; Taliani, S.; Trincavelli, M.L.; Montali, M.; Martini, C. *Curr. Med. Chem*. **2007**, *14*, 2680-2701.

41. Mellon, S.H.; Griffin, L.D. *Endocr. Res.* **2002**, *28*, 463-468.

42. Brambilla, F.; Biggio, G.; Pisu, M.G.; Bellodi, L.; Perna, G.; Bogdanovich-Djukic, V.; Purdy, R.H.; Serra, M. *Psychiatry Res*. **2003**, *118*, 107-116.

43. Marazziti, D.; Dell'Osso, B.; Baroni, S.; Masala, I.; Di Nasso, E.; Giannaccini, G.; Conti, L. *Life Sci*. **2005**, *77*, 3268-3275.

44. Dell'Osso, L.; Da Pozzo, E.; Carmassi, C.; Trincavelli, M.L.; Ciapparelli, A.; Martini, C. *Psychiatry Research*. **2010**, *177*, 139-143.

45. Beurdeley-Thomas, A.; Miccoli, L.; Oulard, S.; Dutrillaux, B.; Poupon, M. F.; *J. Neurooncol.* **2000**, *46*, 45-56.

46. Cappelli, A.; Anzini, M.; Vomero, S.; De Benedetti, P. G.; Menziani, M. C.; Giorgi, G.; Manzoni, C. *J. Med. Chem.,* **1997**, *40*, 2910-2921.

47. Matarrese, M.; Moresco, R. M.; Cappelli, A.; Anzini, M.; Vomero, S.; Simonelli, P.; Verza, E.; Magni, F.; Sudati, F.; Soloviev, D.; Todde, S.; Carpinelli, A.; Kienle, M. G.; Fazio, F. *J. Med. Chem*., **2001**, *44*, 579-585.

48. Cappelli, A.; Mohr, P. G.; Gallelli, A.; Giuliani, G.; Anzini, M.; Vomero, S.; Fresta, M.; Porcu, P.; Maciocco, E.; Concas, A.; Biggio, G.; Donati, A.; *J. Med. Chem.,* **2003**, *46*, 3568-3571.

49. Anzini, M.; Cappelli, A.; Vomero, S.; Seeber, M.; Menziani, M. C.; Langer, T.; Hagen, B.; Manzoni, C.; Bourguignon, J. J. *J. Med. Chem.,* **2001**, *44*, 1134-1150.

50. Taliani, S.; Pugliesi, I.; Da Settimo, F. *Curr. Top. Med. Chem.* **2011**, *11*, 860−886.

51. Da Settimo, F.; Simorini, F.; Taliani, S.; La Motta, C.; Marini, A. M.; Salerno, S.; Bellandi, M.; Novellino, E.; Greco, G.; Cosimelli, B.; Da Pozzo, E.; Costa, B.; Simola, N.; Morelli, M.; Martini, C. *J. Med. Chem*. **2008**, 51, 5798−5806.

52. Campiani, G.; Nacci, V.; Fiorini, I.; De Filippis, M. P.; Garofalo, A.; Ciani, S. M.; Greco, G.; Novellino, E.; Williams, D. C.; Zisterer, D. M.; Woods, M. J.; Mihai, C.; Manzoni, C.; Mennini, T. *J. Med. Chem*. **1996**, 39, 3435−3450.

53. Trapani, G.; Franco, M.; Ricciardi, L.; Latrofa, A.; Genchi, G.; Sanna, E.; Tuveri, F.; Cagetti, E.; Biggio, G.; Liso, G. *J. Med. Chem*. **1997**, *40*, 3109-3118.

54. Serra, M.; Madau, P.; Chessa, M.F.; Caddeo, M.; Sanna, E.; Trapani, G.; Franco, M.; Liso, G.; Purdy, R.H.; Barbaccia, M.L.; Biggio, G. Br. *J. Pharmacol*. **1999**, *127*, 177-187.

55. Okubo, T.; Yoshikawa, R.; Chaki S.; Okuyama S.; Nakazato A. *Bioorg. Med. Chem*. **2004**, *12*, 423-438.

56. Okuyama, S.; Chaki, S.; Yoshikawa, R.; Ogawa, S.I.; Suzuki, Y.; Okubo, T.; Nakazato, A.; Nagamine, M.; Tomisawa, K. *Life Sci*. **1999**, *64*, 1455-1464.

57. Culty, M.; Silver, P.; Nakazato, A.; Gazouli, M.; Li, H.; Muramatsu, M.; Okuyama, S.; Papadopoulos, V. *Drug Develop. Res.* **2001**, *52*, 475-484.

58. Selleri, S., Bruni, F., Costagli, C., Costanzo, A., Guerrini, G., Ciciani, G., Costa, B., Martini, C. *Bioorg. Med. Chem.* **2001**, *9*, 2661-2671.

59. Primofiore, G.; Da Settimo, F.; Taliani, S.; Simorini, F.; Patrizi, M.P.; Novellino, E.; Greco, G.; Abignente, E.; Costa, B.; Chelli, B.; Martini, C. *J. Med. Chem.* **2004**, 47, 1852-1855.

60. Venneti, S.; Lopresti, B.J.; Wiley, C.A. *Prog. Neurobiol*., **2006**, *80*, 308**–**322.

61. Zhang M.R., Ogawa M., Ito T., Noguchi J., Kumata K., Okauchi T., Suhara T., Suzuki K. *J. Med. Chem*. **2006,** *49*, 2735-2742.

62. Doorduin J., Klein H.C., Dierckx R.A., James M., Kassiou M.; De Vries E. F. *Molecular imaging and biology* **2009**, *11*, 386-398.

63. Chaveau, F.; Boutin, H.; Van Camp, N.; Dollè, F.; Tavitian, B. *Eur. J. Nucl. Med. Mol. Imaging*. **2008**, *35*, 2304-2319.

64. Petit-Taboue, M.C.; Baron, J.C.; Barre, L.; Travere, J.M.; Speckel, D.; Camsonne, R. *Eur J Pharmacol.* **1991**, *200*, 347-351.

65. Shah, F.; Hume, S.P.; Pike, V.W.; Ashworth, S.; McDermott, J. *Nucl. Med. Biol.* **1994**, *21*, 573-581.

66. Venneti, S.; Wiley, C.A. *Prog. Neurobiol.* **2006**, *80*, 308-322.

67. Elizarov, A.M. *Lab on Chip* **2009**, *9*, 1326–1333.

68. Lu, S.; Pike V.W. *Curr. Radiopharmaceuticals* **2009**, *1*, 49–55

69. Pascali, C.; Luthra, S.K.; Pike, V.W.; Price, G.W.; Ahier, R.G.; Hume, S.P.; Myers, R.; Manjil, L.; Cremer J.E. *Appl. Radiat. Isot*. **1990**, *41*, 477−482.

70. Chun, J.H. Morse, C.L.; Chin, F.T.; Pike, V.W. *Chem. Commun*. **2013**, *49*, 2151-2153.

71. *J. Chem. Educ* **2003**, *80* (6), 679.

72. Mc Graw-Hill, Nucleophilic aromatic substitutions, A1-A5.

73. Castellano S.; Taliani S.; Milite C.; Pugliesi I.; Da Pozzo E.; Rizzetti E.; Bendinelli S.; Costa B.; Cosconati S.; Greco G.; Novellino E.; Sbardella G.; Stefancich G.; Martini C.; Da Settimo F.; *J. Med. Chem.,* **2012,** *55*, 4506−4510